

CACTUS

Paulo Afonso

Maxwell Chertok

Juan Lizarazo

Peter Marleau

Sho Maruyama

Mani Tripathi

John Stilley

A UC-Davis Facility

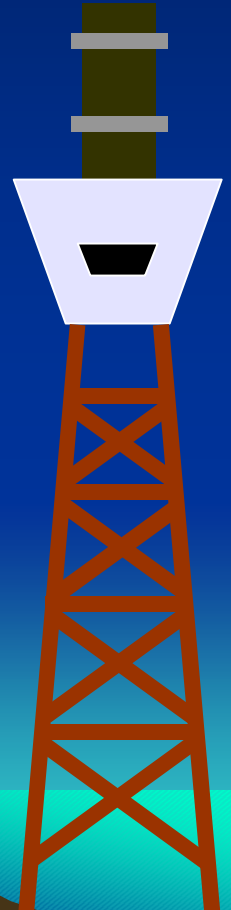
Senior Engineer: Britt Holbrook

Junior Specialist: Tiffany Landry.

Undergrads: John Felde, Cherie Williams, Sasha Laundry, Emily Rostel.

Technical Assistants: John Linn, Joe Trad.

Mani Tripathi, C2CR, Prague, Sept 9,
2005.



Outline

- Solar Two facility and CACTUS.
 - Instrument:
 - 250 channel (effective) camera.
 - Simulations and Calibrations
 - optics & noise
 - energy response
 - Crab
 - The Dark Matter problem & Draco
 - Data & Preliminary analysis.
- Future prospects - Dwarf spheroid survey.

The Solar 2 Heliostat Array

Located 15 miles
outside Barstow,
CA

Over 1,900 42m^2
heliostats. The
largest array in the
world.

We have ~ 160
heliostats in the
FOV of our
camera.

Collection area
 $\sim 64,000\text{ m}^2$.

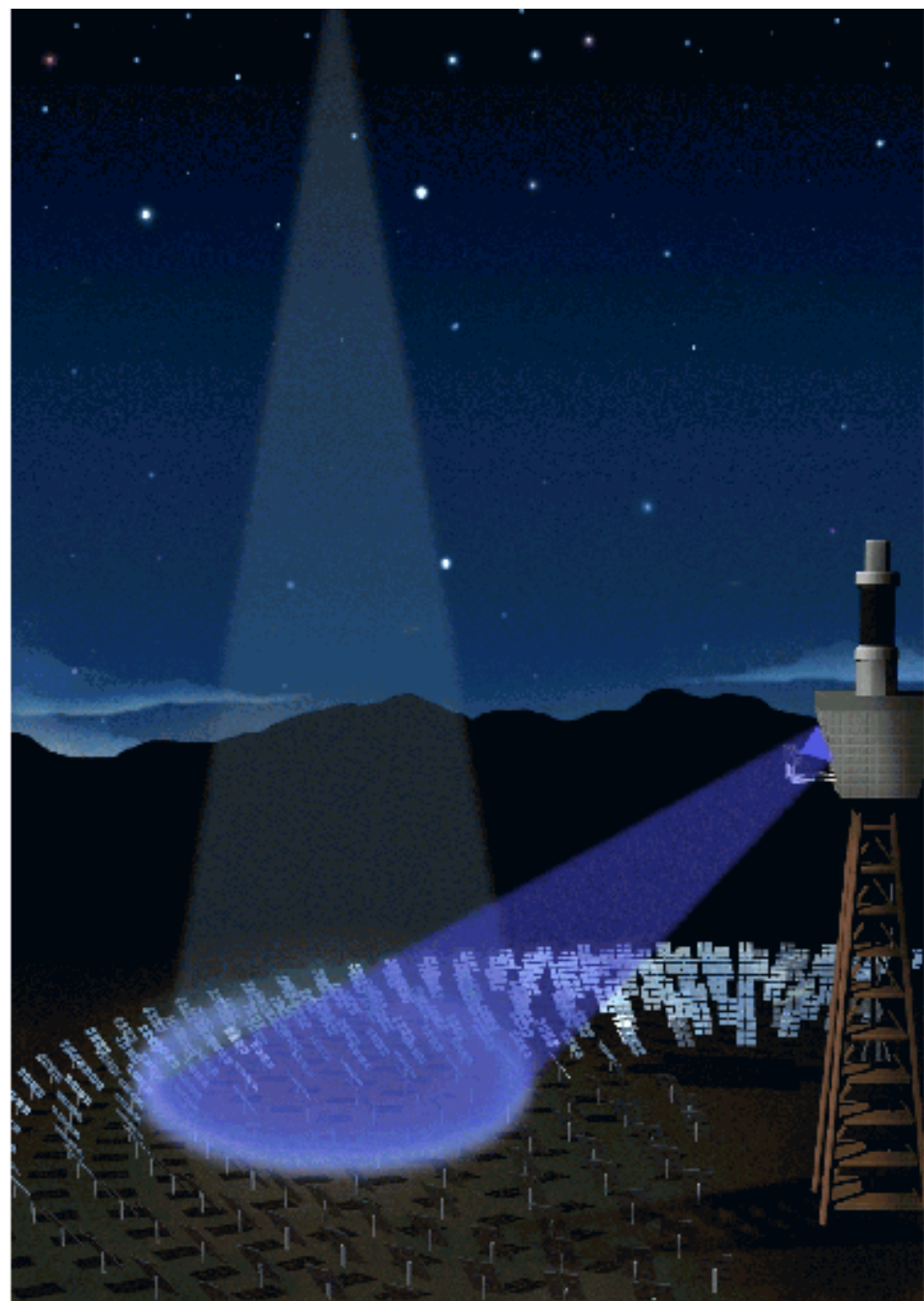


Air Cherenkov

Heliostat arrays offer large collection areas that are not possible with imaging telescopes. Solar Two is the only field large enough to contain the entire Cherenkov light pool.

Utilizing existing arrays is a highly cost-effective method of constructing large area telescopes.

Solar Two was abandoned in 1998 after a successful run as a pilot plant/technology demonstration project.



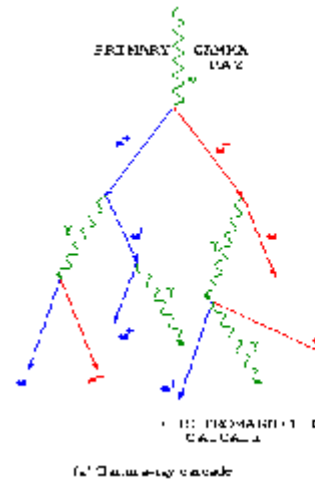
Detection Technique

Electromagnetic showers produce a coherent and compact ring-like Cerenkov wavefront.

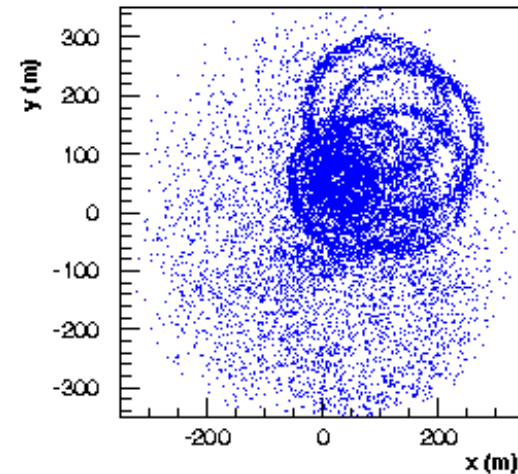
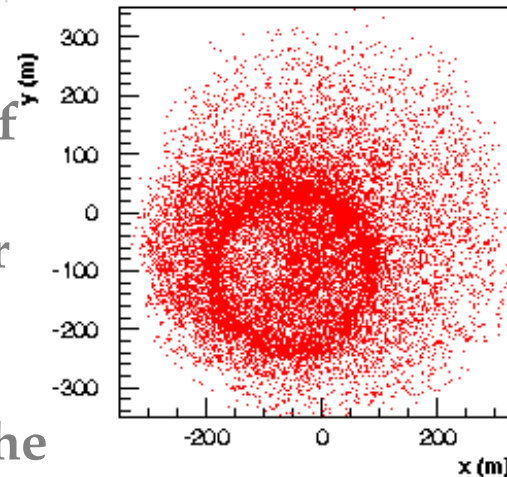
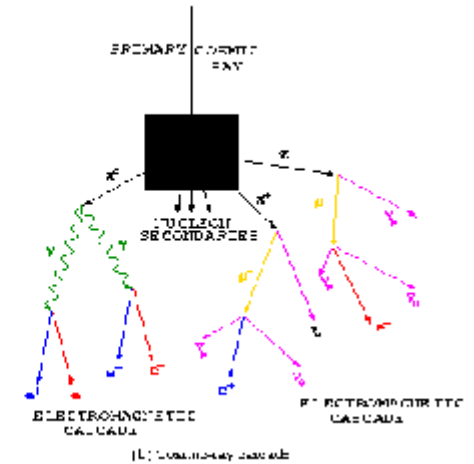
Proton showers consist of EM sub-showers due to neutral pions and/or individual rings due to muons.

Core diameter of the light pool is nearly independent of the primary particle energy (refractive index in the upper atmosphere is very close to unity and the radiating particles rapidly fall below the Cerenkov threshold).

Gamma



Proton




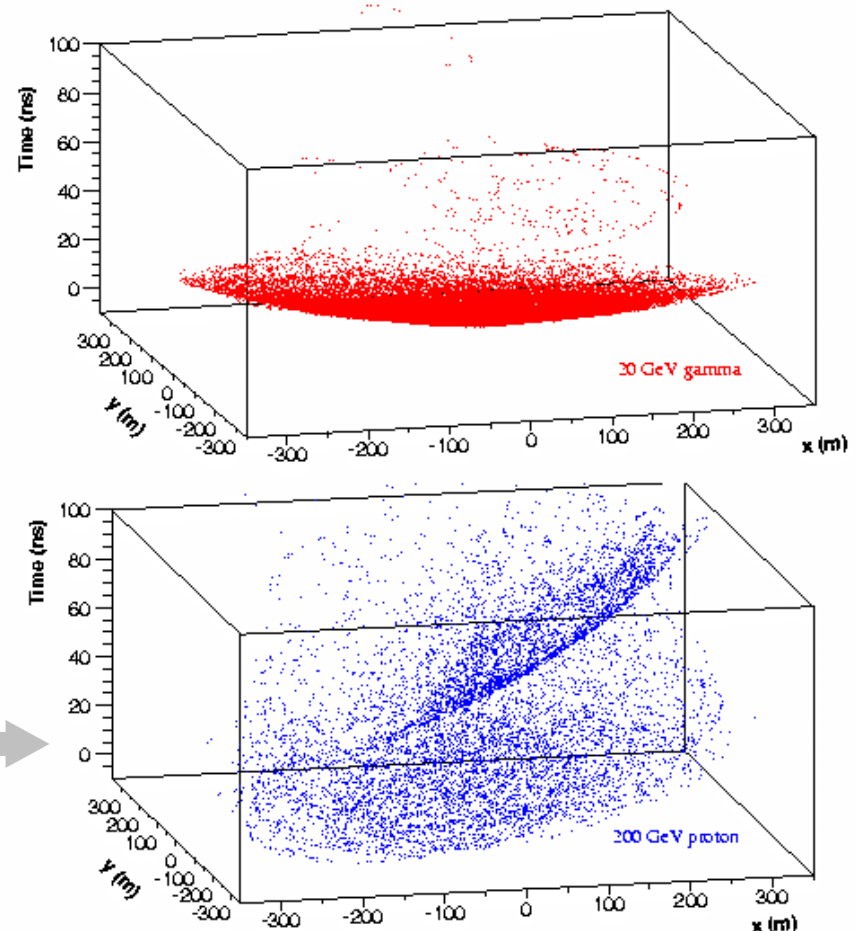
Detecting the Cherenkov Light

Ground based telescopes attempt to sample a fraction of the core light pool which is $\sim 200 - 250$ m in diameter.

Good energy resolution demands a high photon detection efficiency. Night-sky background is in the range of $\sim 3-6 \times 10^{12}$ photons/m²/s/sr.

Temporal coherence ($\sim 3-5$ ns) of the Cerenkov wavefront allows for sharp coincidences between camera elements.

CACTUS can exploit differences in time-structure between gamma and proton showers. 



80 channel camera

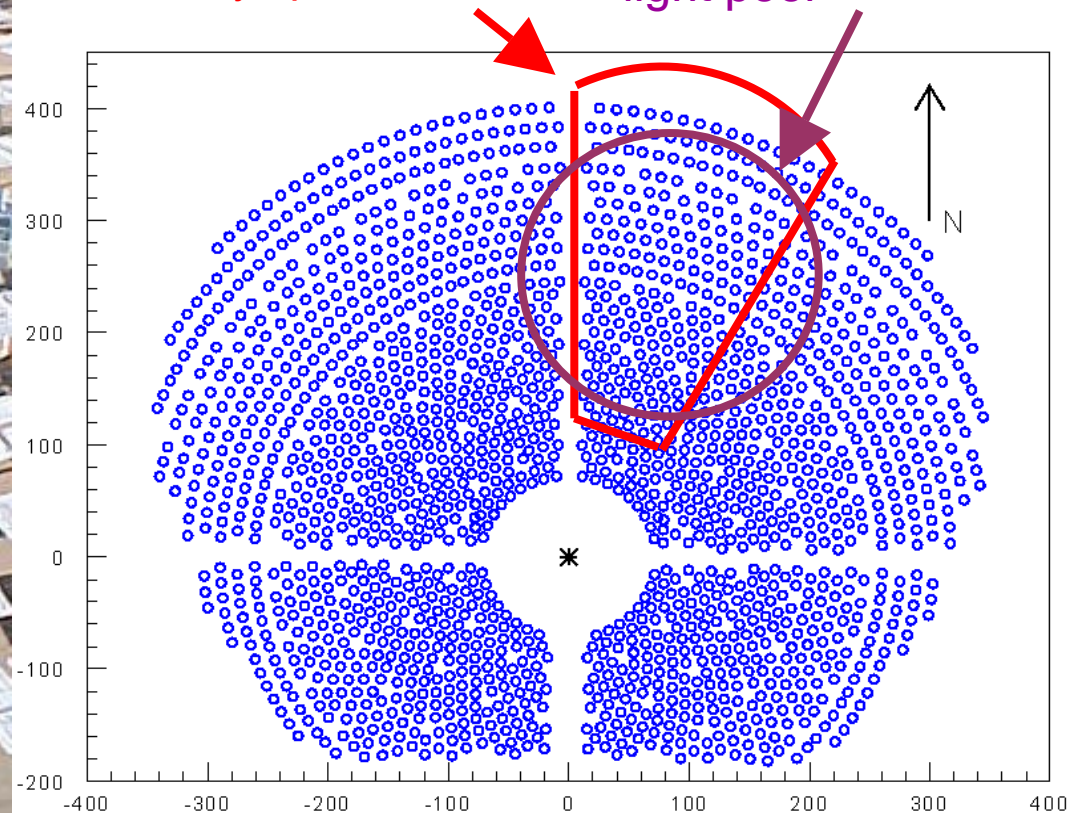


Heliostat Field

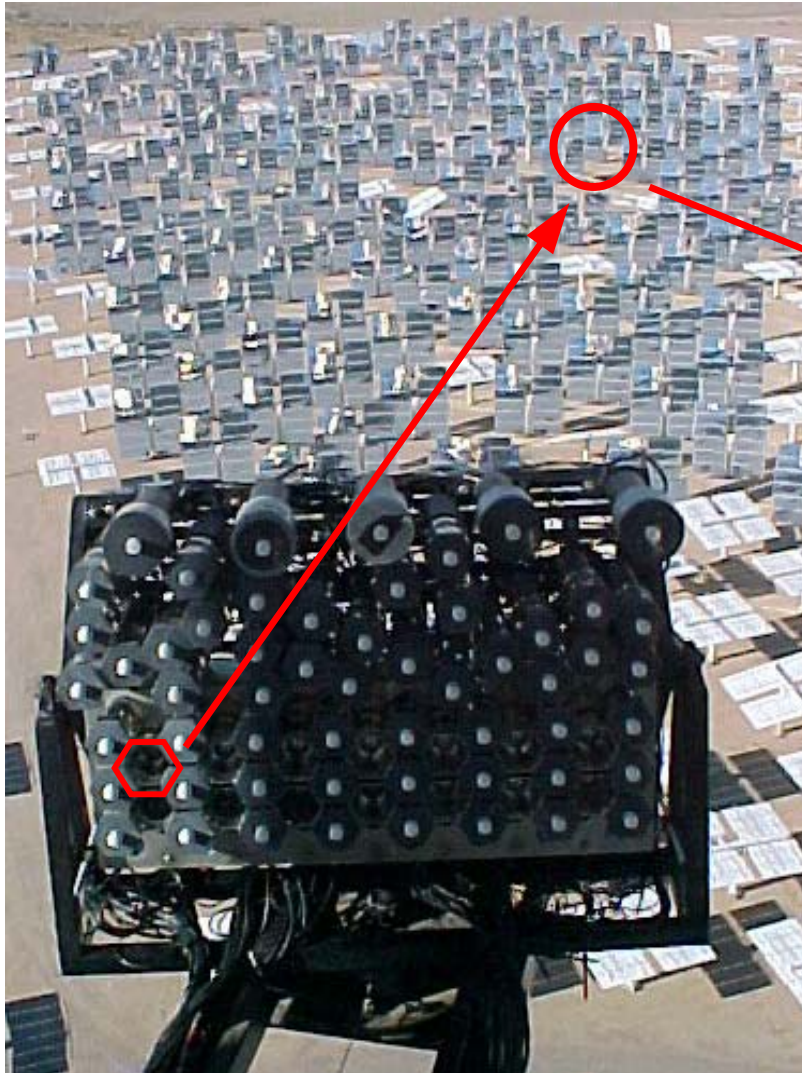
Part of the field being used. 160 heliostats* available. 140 used in this campaign.

*limited by aperture

CACTUS is capable of collecting nearly the entire Cherenkov light pool

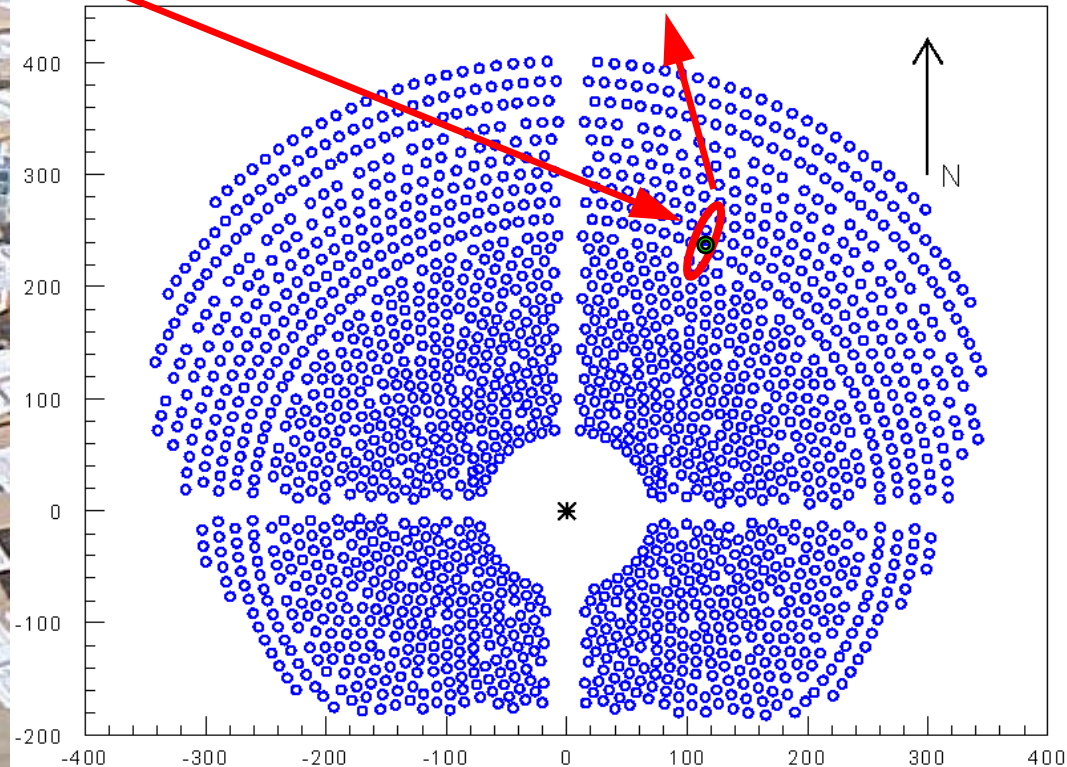
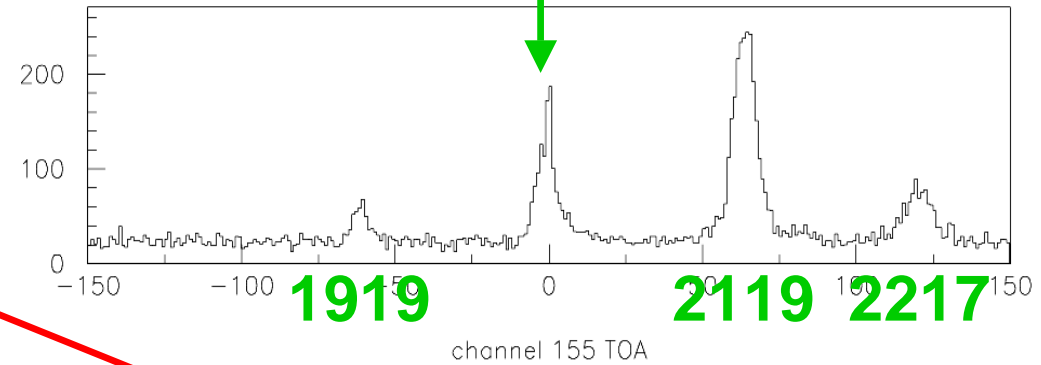


80 channel camera

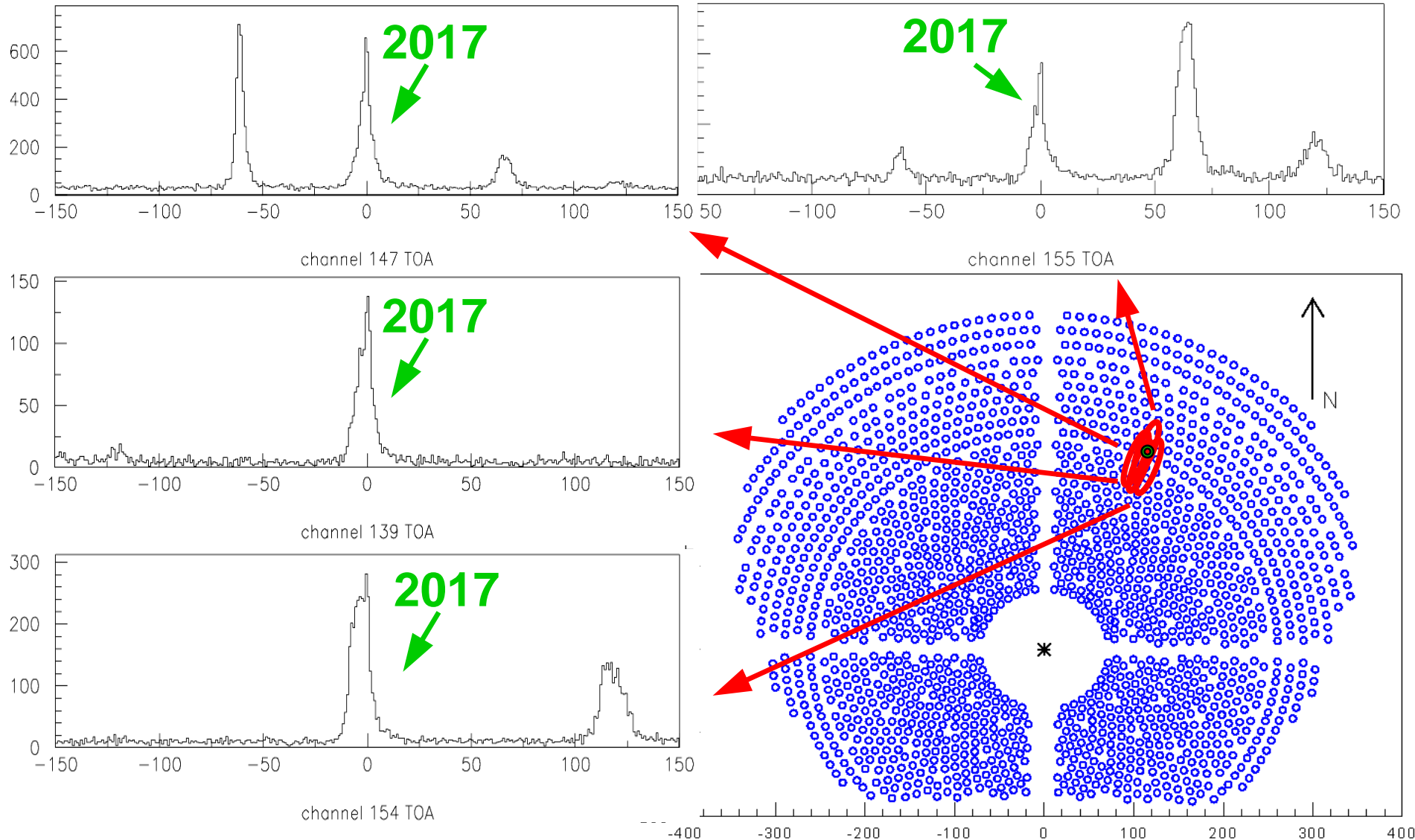


Time expected for heliostat 2017.

Heliostat Field

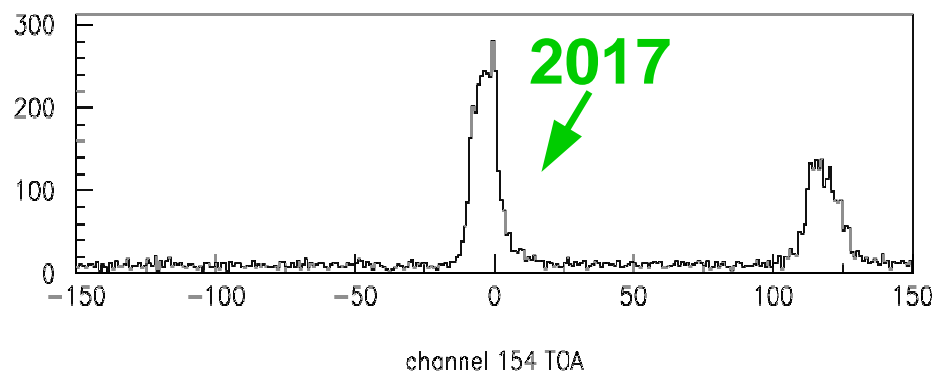
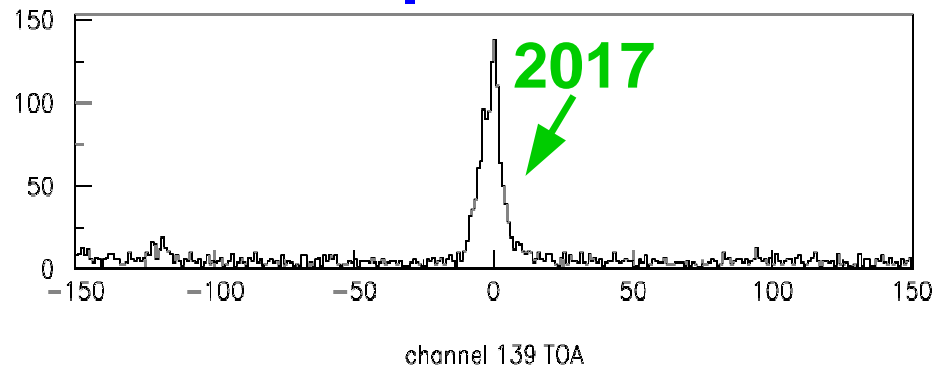


Channel Multiplicity

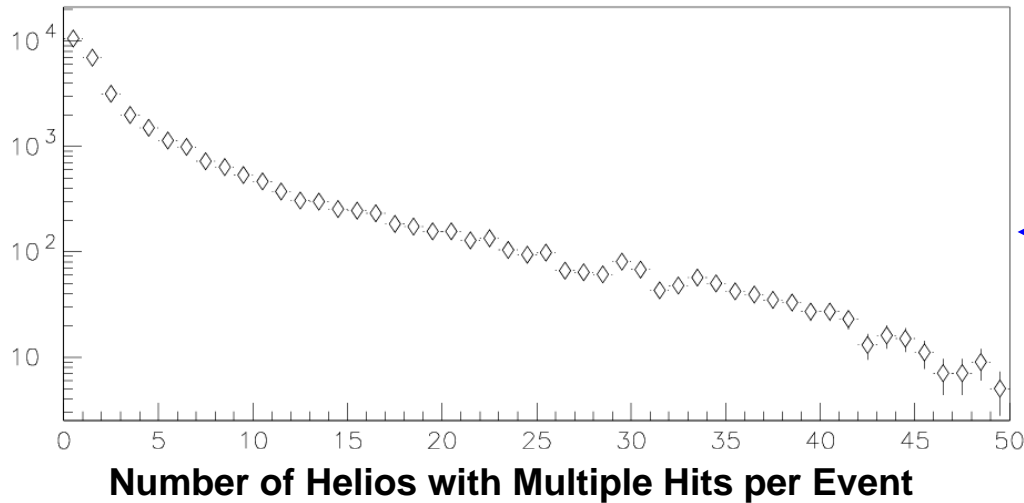


Heliostat Multiplicity

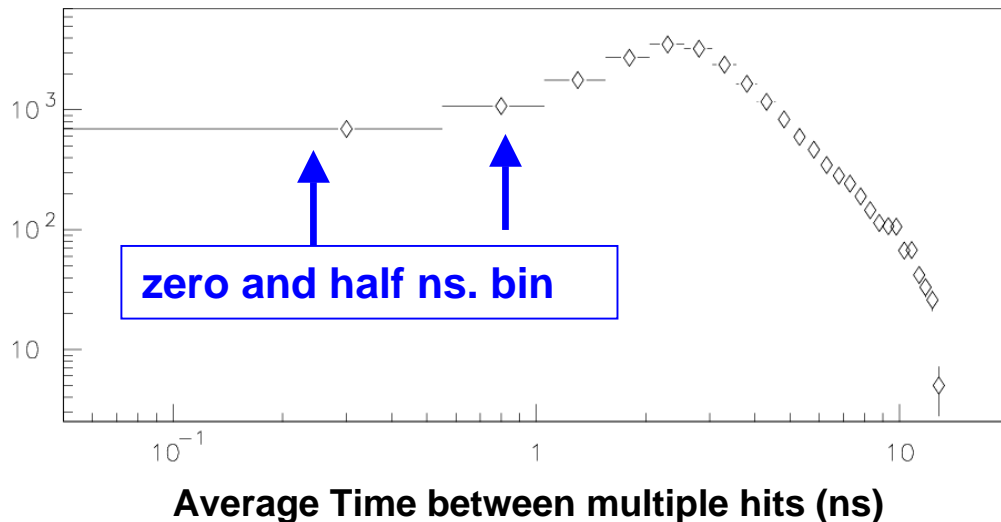
- Heliostat 2017 is covered by 4 PMTS
- This allows us to record multiple hits on each heliostat with full two-pulse resolution



Heliostat Multiplicity

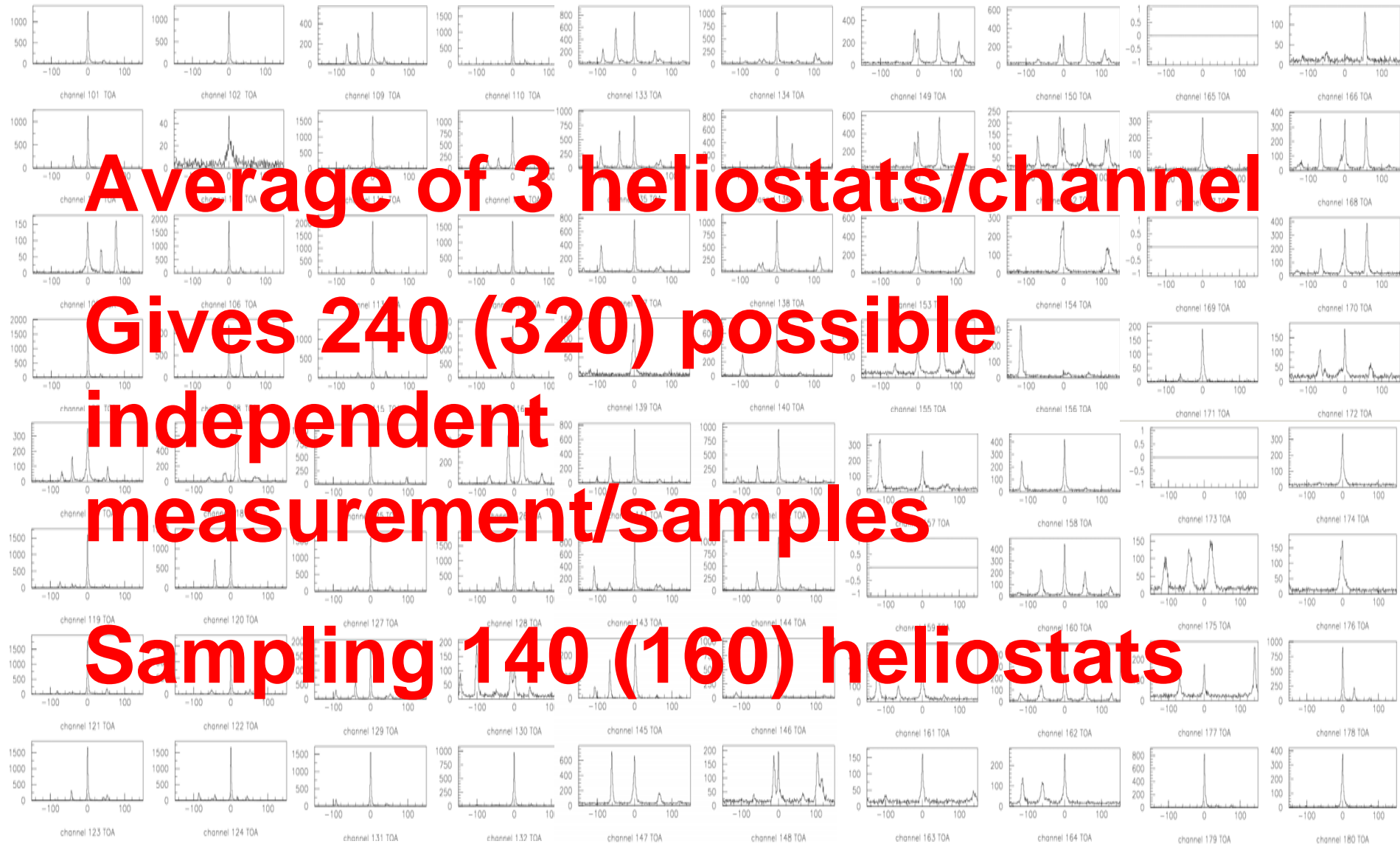


Most events contain multiple hits in each heliostat.



We can record multiple hits with 0.5 ns resolution without any pile-up.

Heliostat Multiplicity



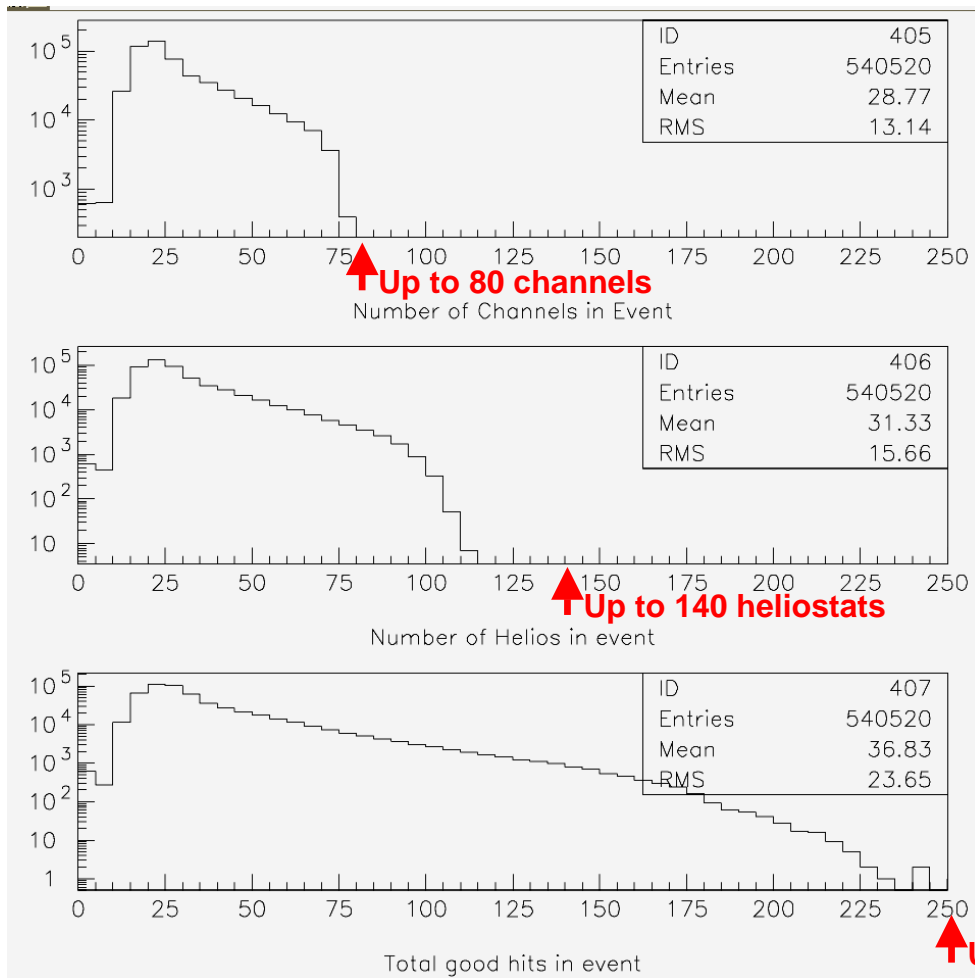
Average of 3 heliostats/channel

Gives 240 (320) possible

independent measurement/samples

Sampling 140 (160) heliostats

Heliostat Multiplicity



Dynamic range if 80 channels mapped to 80 heliostats.

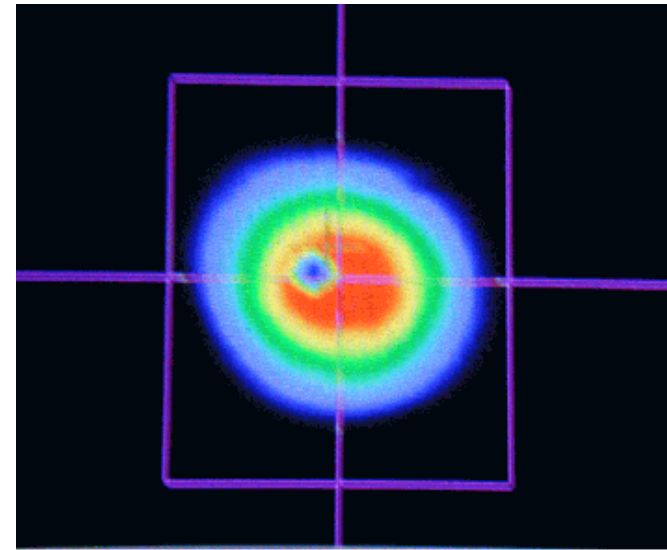
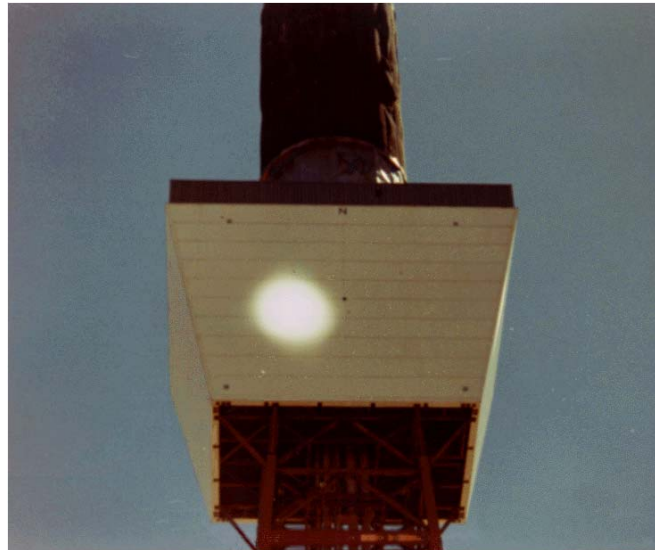
Dynamic range gained by using more than 80 heliostats.

Dynamic range using heliostat multiplicity.

Heliostat Alignment and MC Calibration

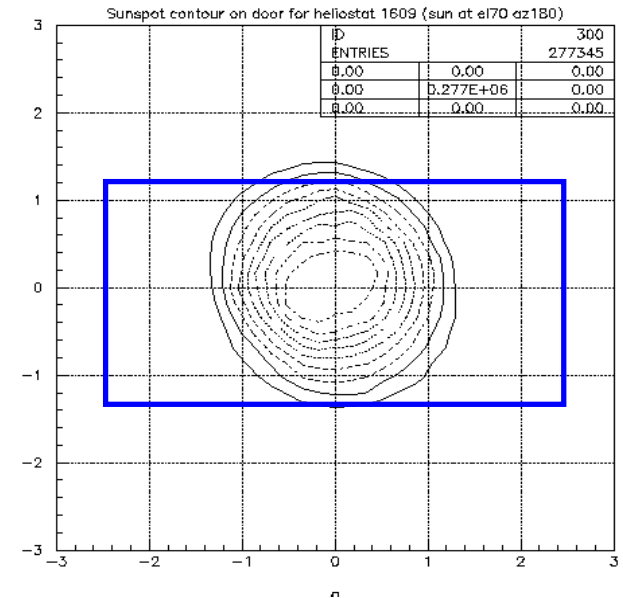
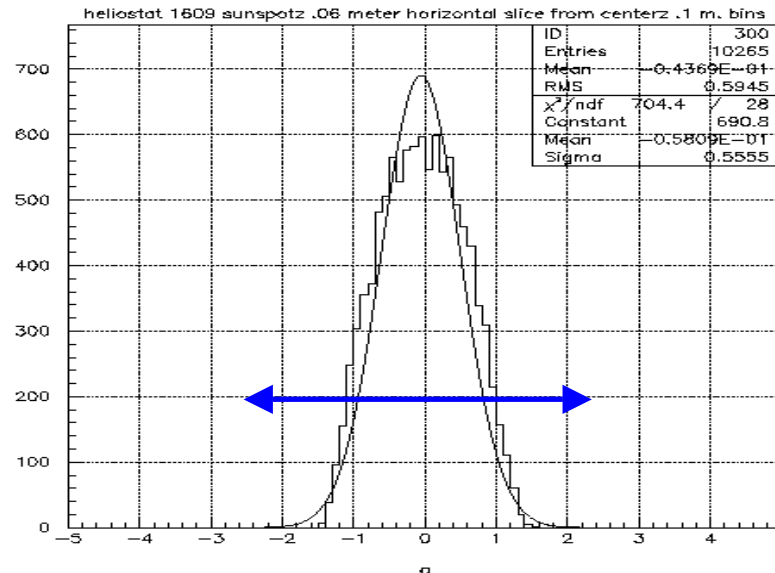
The heliostats are aligned using a sunspot projected on the tower face.

An infrared CCD camera is used to measure the sun spot and maximize the brightness at the core.



Simulated Sunspots

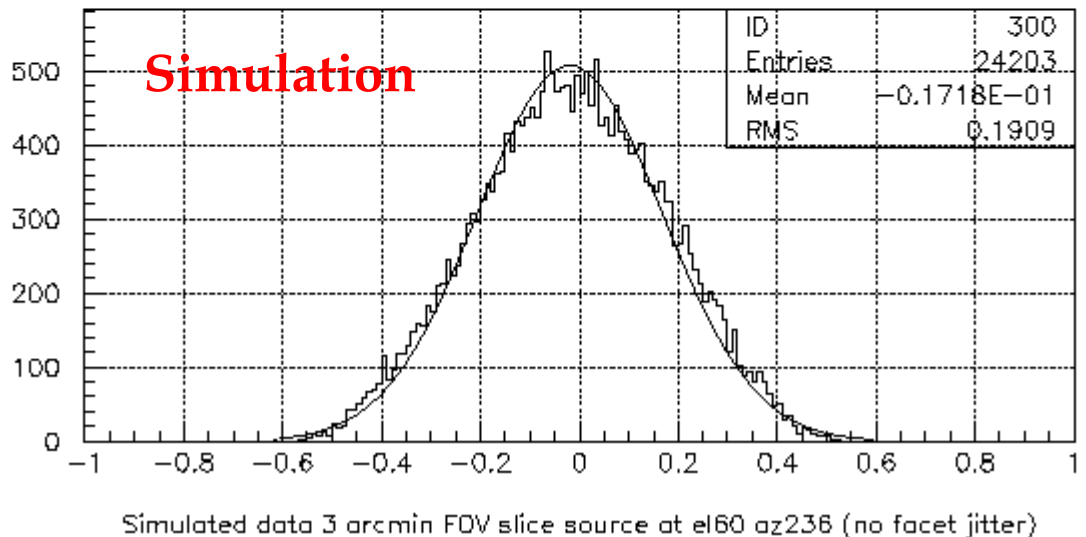
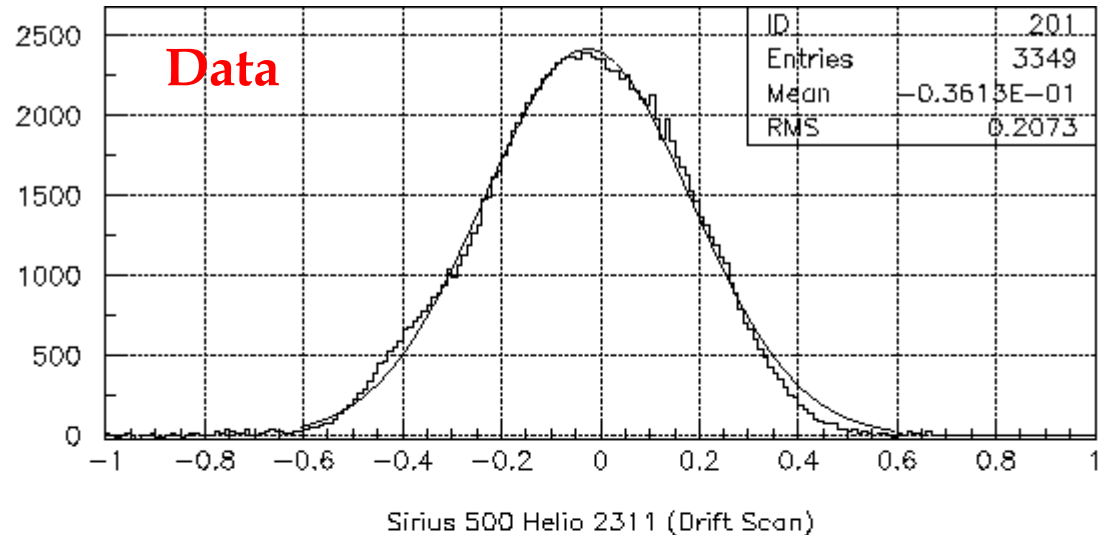
Heliostat facet parameters were optimized to match the CCD images



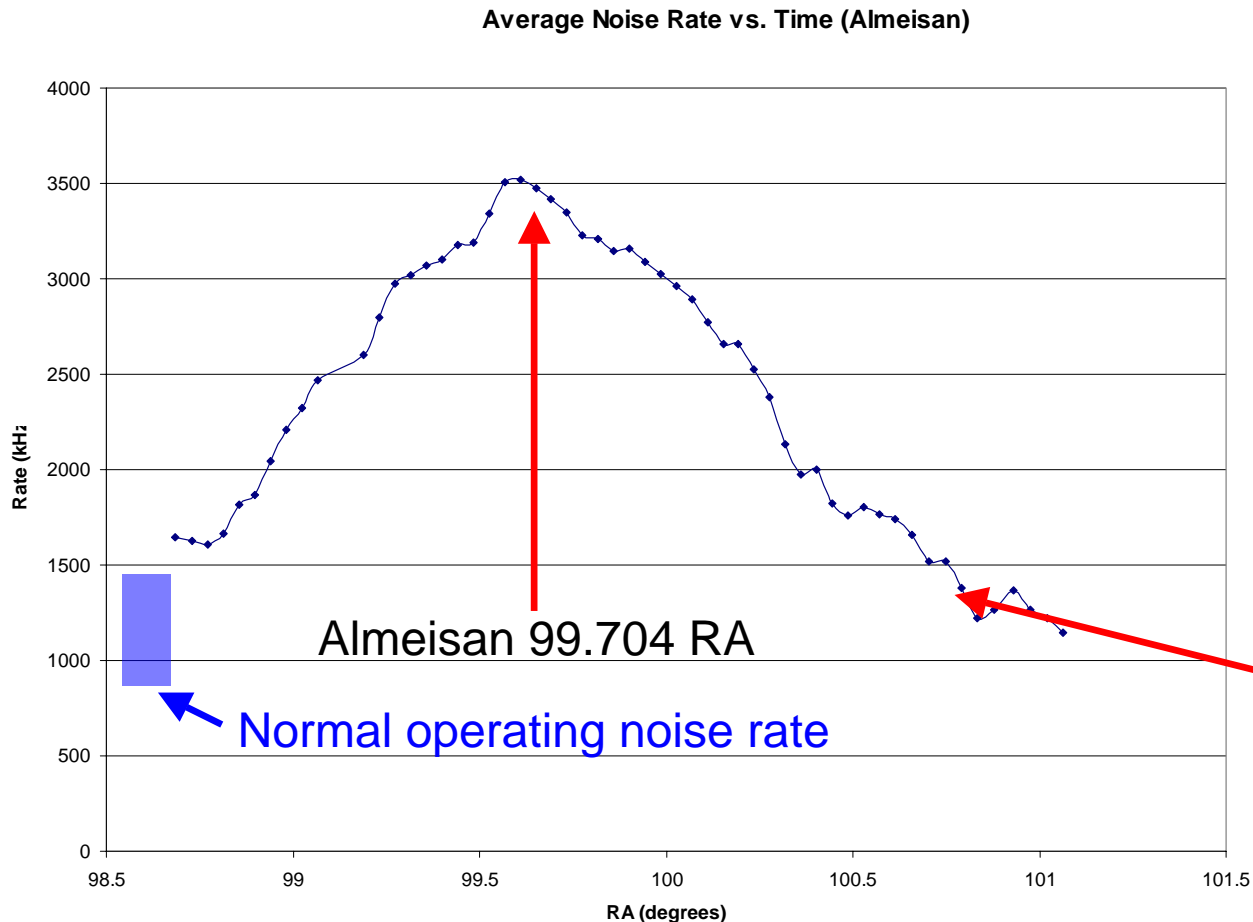
Calibrations and Simulation

Calibrating with starlight: Drift scan of Sirius

Drift scan of Sirius
across one heliostat
compared with a
detailed simulation
of all the optical
elements involved.



Almeisan Noise Drift Scan



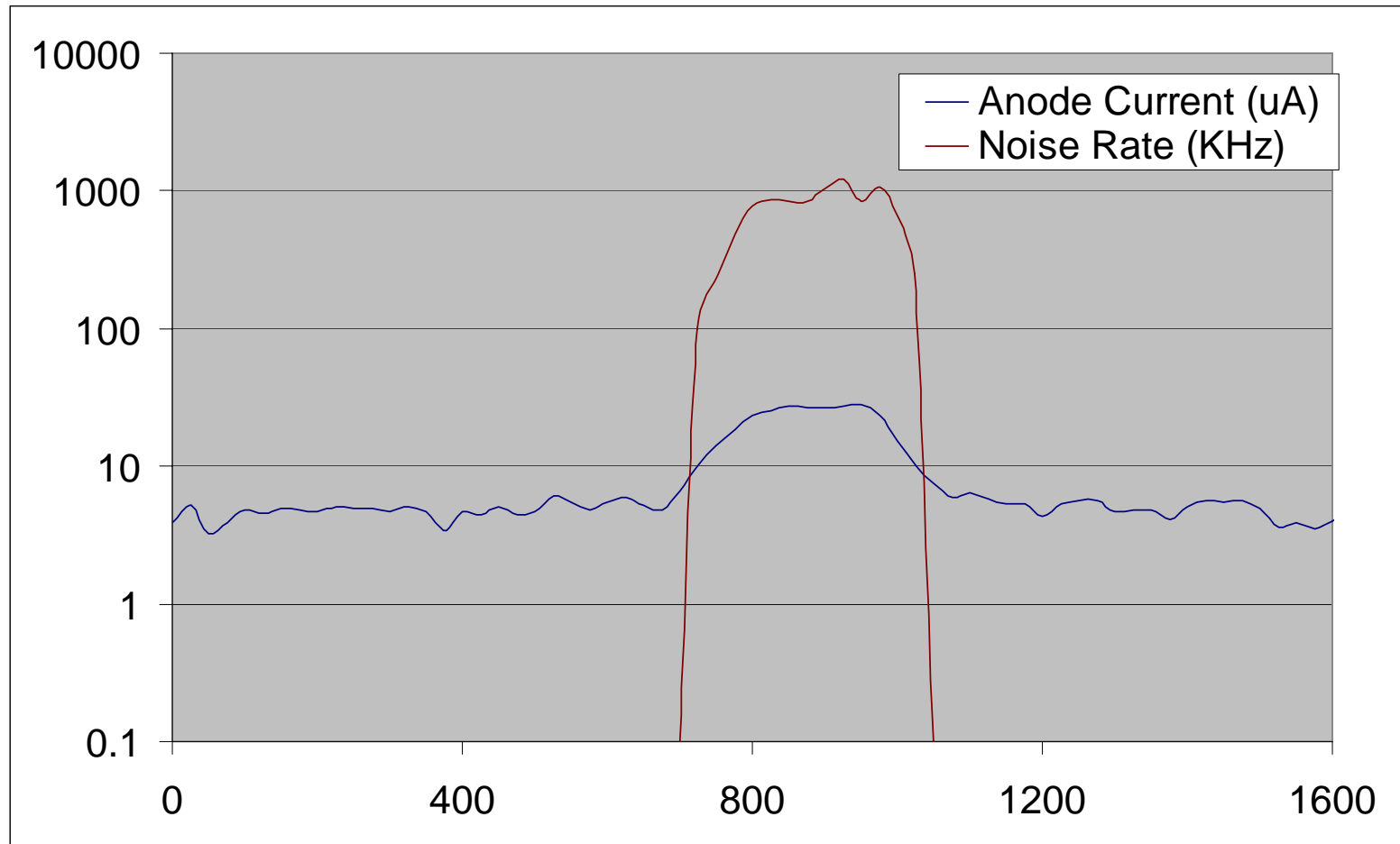
Background Noise Rates as the star Almeisan drifts across our field of view.

Rates are calculated from noise regions of 2 μ sec tdc window.

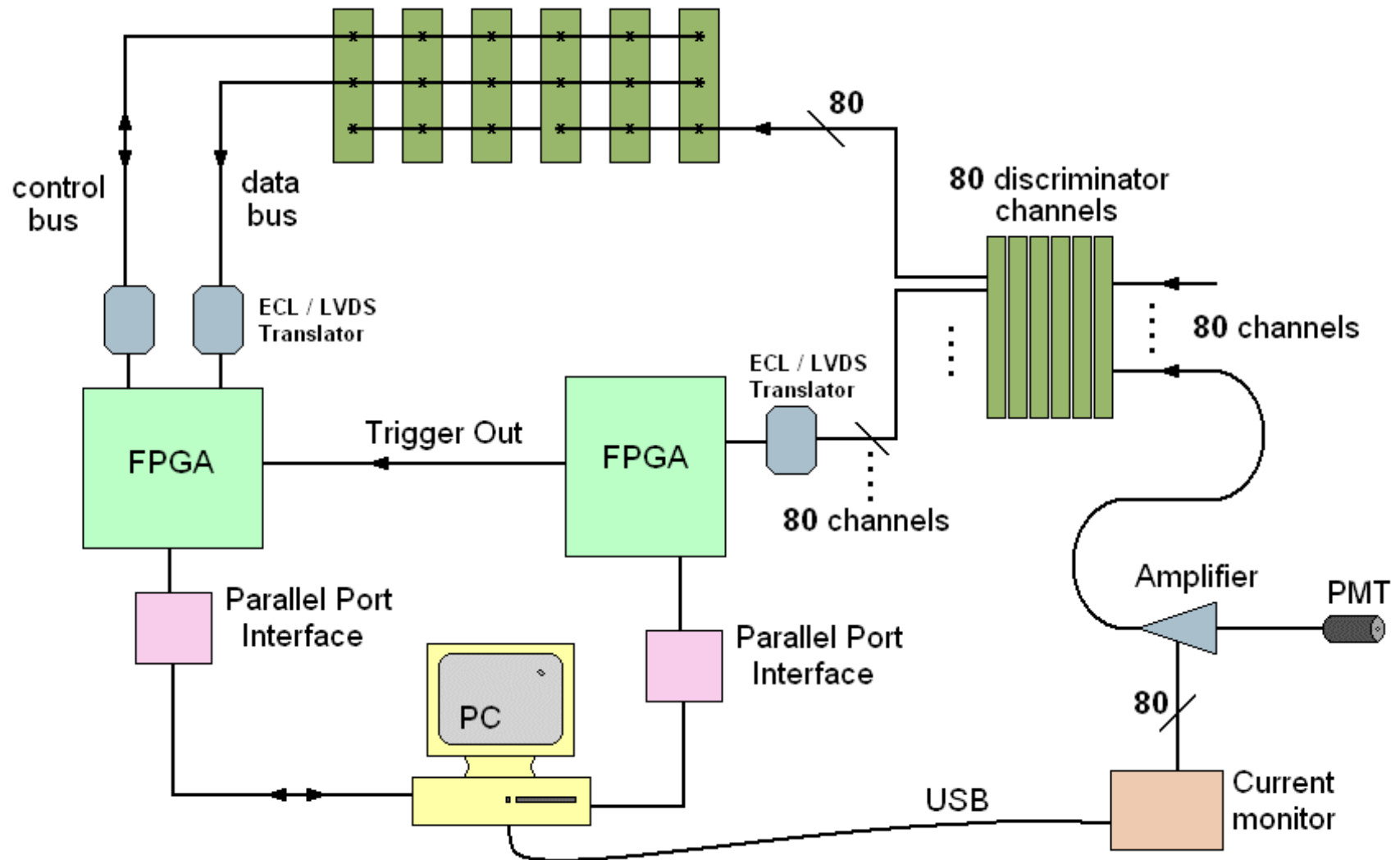
We are within normal noise rates 1 degree from a neighboring star.
(Almeisan is magnitude 7)

Altair Scan

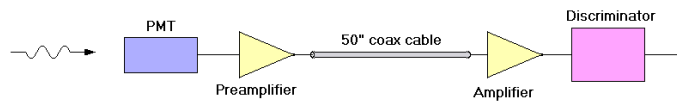
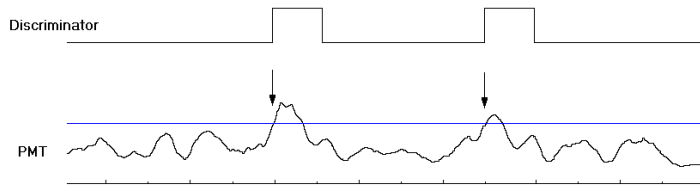
RA = 305.05 Dec = 40.36



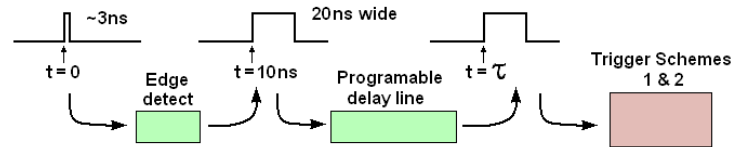
Electronics Chain



Electronics Chain and Trigger

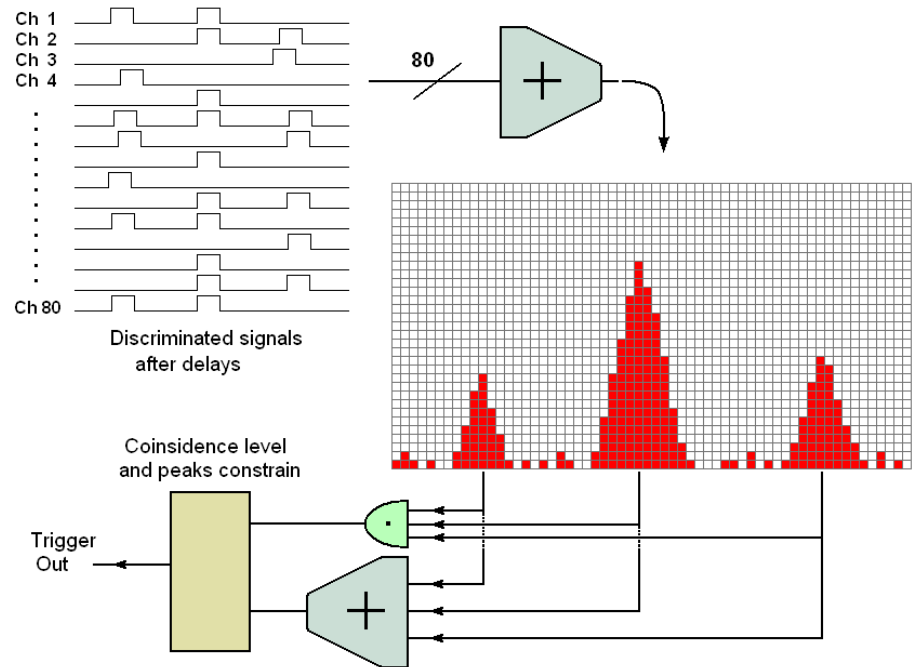


Analog input stage



Trigger Scheme 1: Add all 80 channels and triggers at a given coincidence level.

Trigger Scheme 2: Add all 80 channels and look for a pattern of one central peak with two side peaks, then it ask for a coincidence level to trigger.

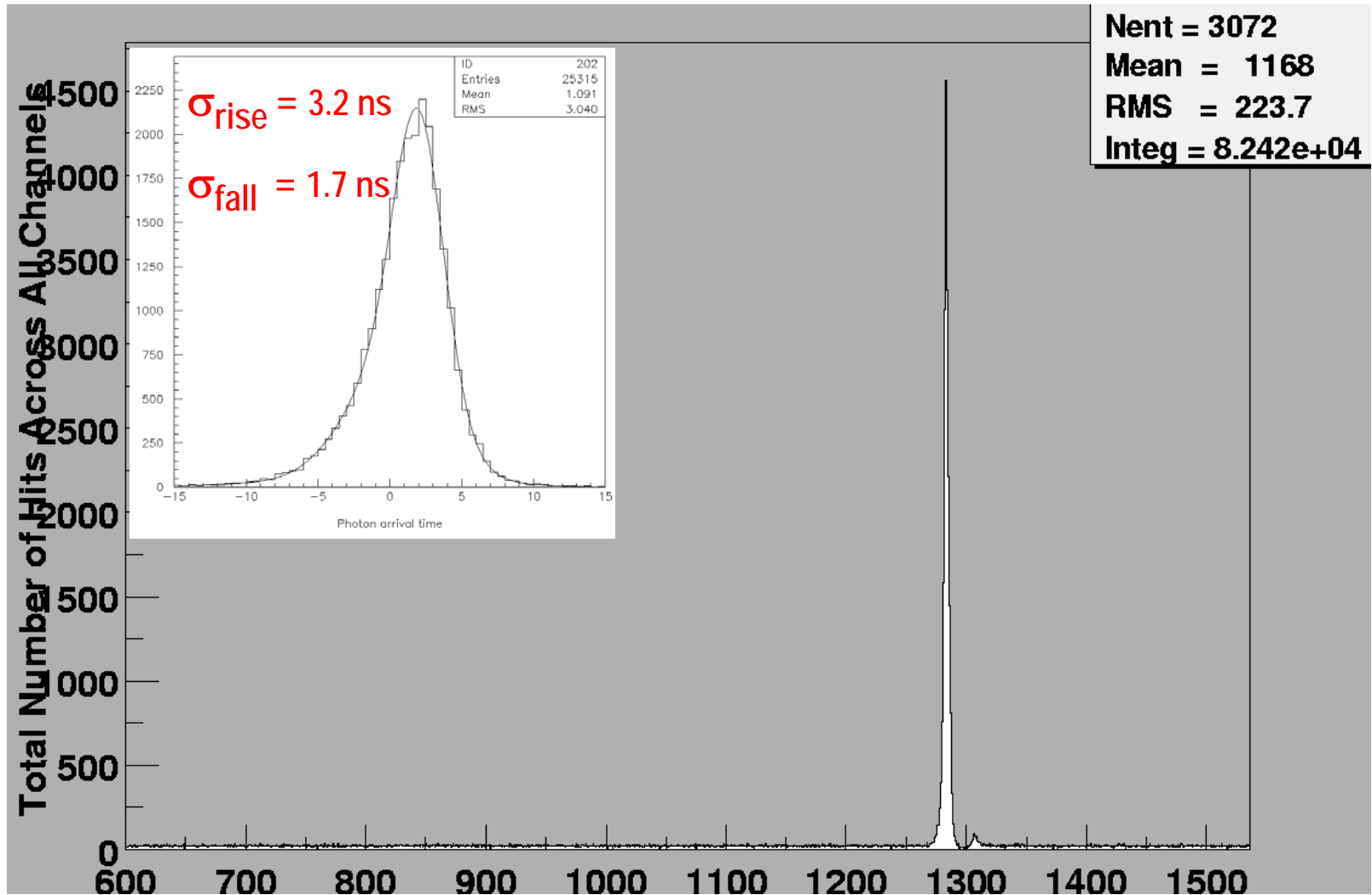


Trigger decision schemes. An FPGA based system allows us to implement several types of trigger.

Data this season was taken with trigger scheme 1, a simple sum of 80 channels.

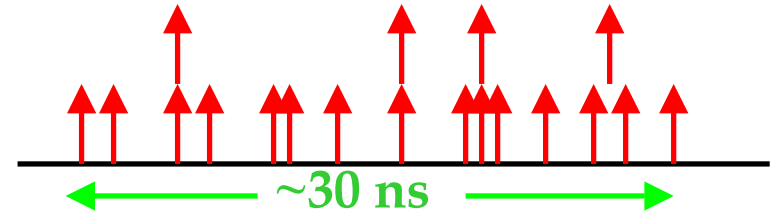
We have also implemented a 3-tap scheme to bring more heliostats into the trigger

Data are recorded in multi-hit TDCs with a time-of-arrival resolution of 0.5 ns. The signal to noise ratio for Cherenkov wavefront detection is excellent.

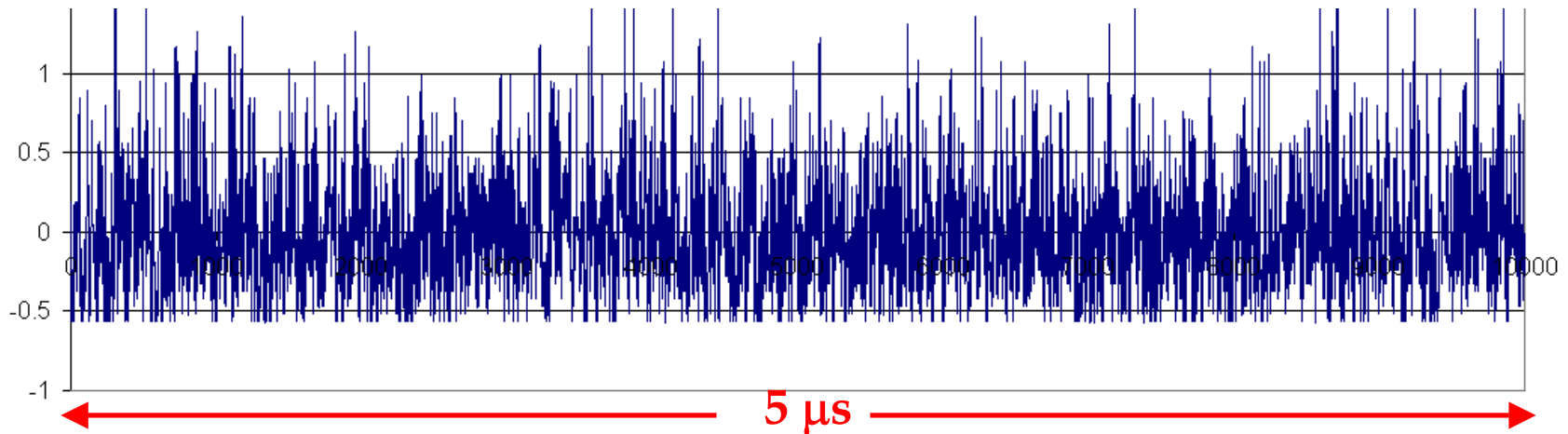


Simulation of Electronic Response

1. Background starlight is simulated by random insertion of photoelectrons. Each p.e. is ascribed a pulse shape based on measurements and with appropriate gain variations.



2. The a.c. component of the piled up p.e.'s is then used as background noise. The agreement with measured noise is excellent.



3. A threshold is applied and digital signals are recorded for comparison with measured rates.

Understanding the NSB

Several simulations were created to understand noise response of our system. Optical and electrical noise were input into a simulated channel and the response was compared to actual data.

... by changing Noise and Gain, we can also match simulated TOT to TOT taken from data.

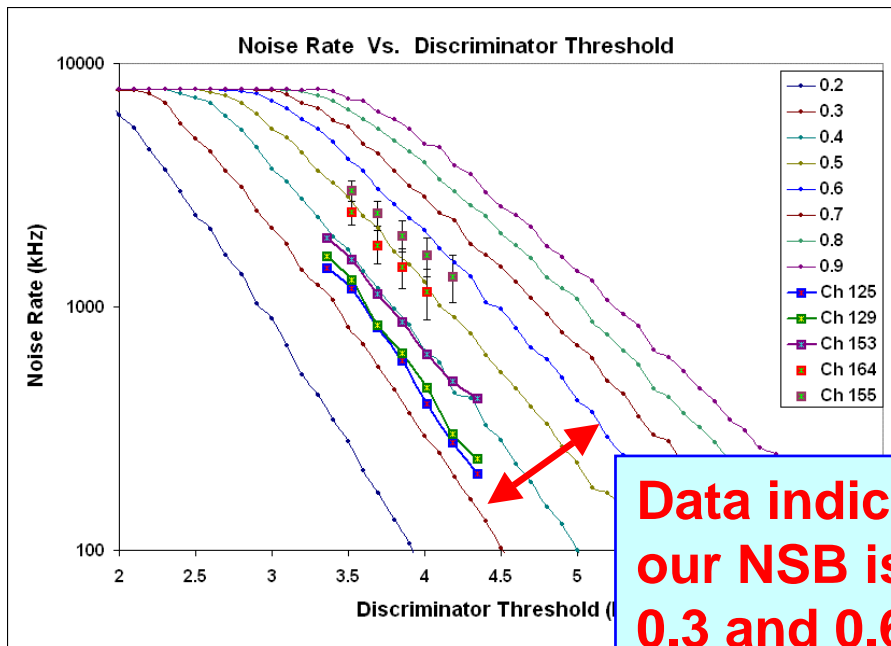
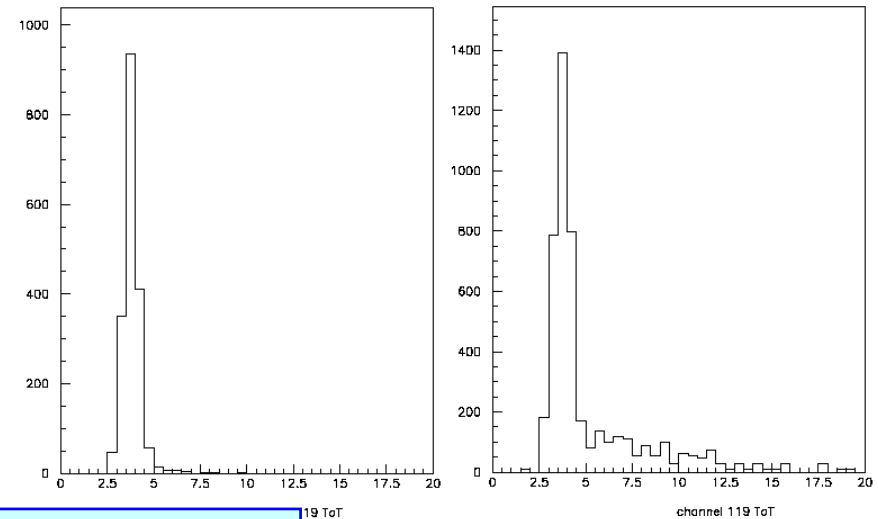


Figure 1. Five typical channels are being fit to different noise curves



Data indicates that our NSB is between 0.3 and 0.6 P.E./ns

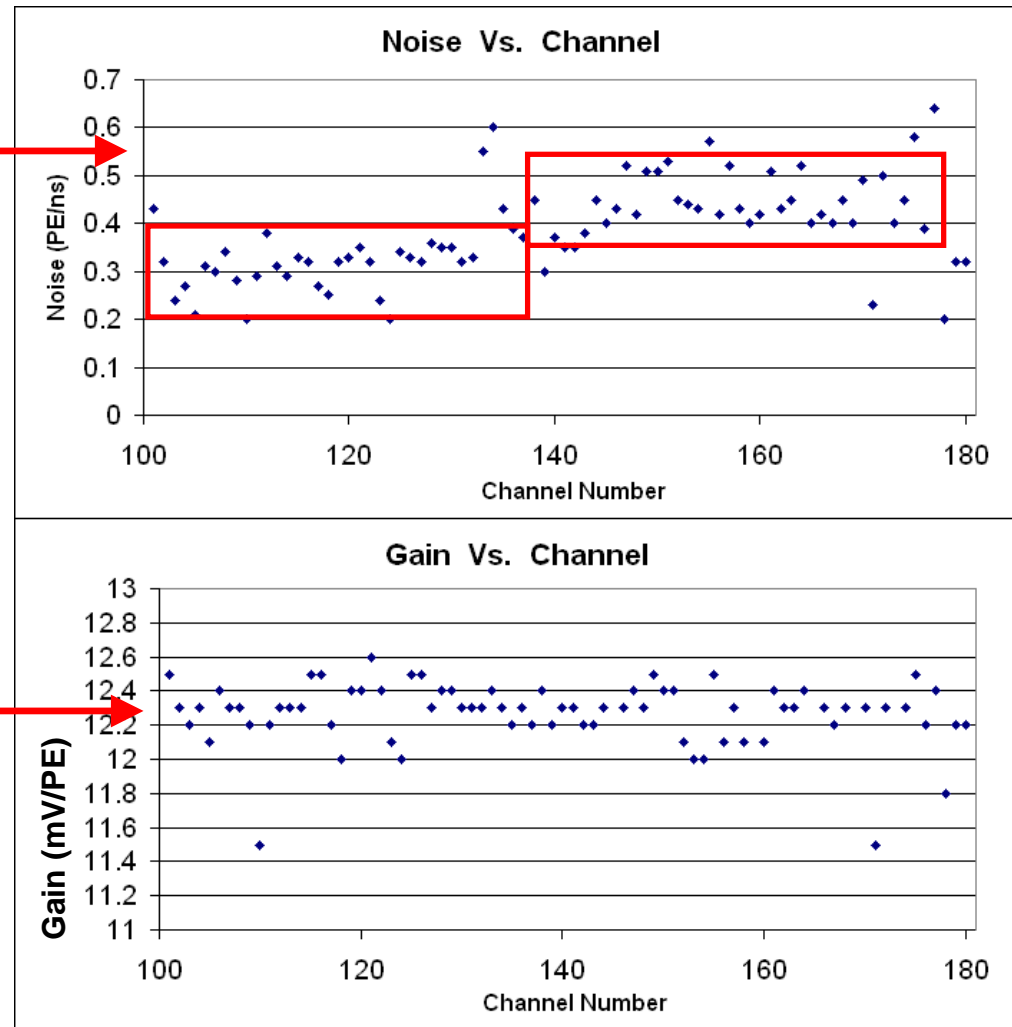
... by changing noise to simulated noise. The plot on the left is pure simulated noise, and the plot on the right is noise plus real showers.

For TOT fitting purposes, only the peak at ~3ns needs to be tuned.

Simulating Night Sky Background

**Simulations indicate that
our threshold is 4.0 PE**

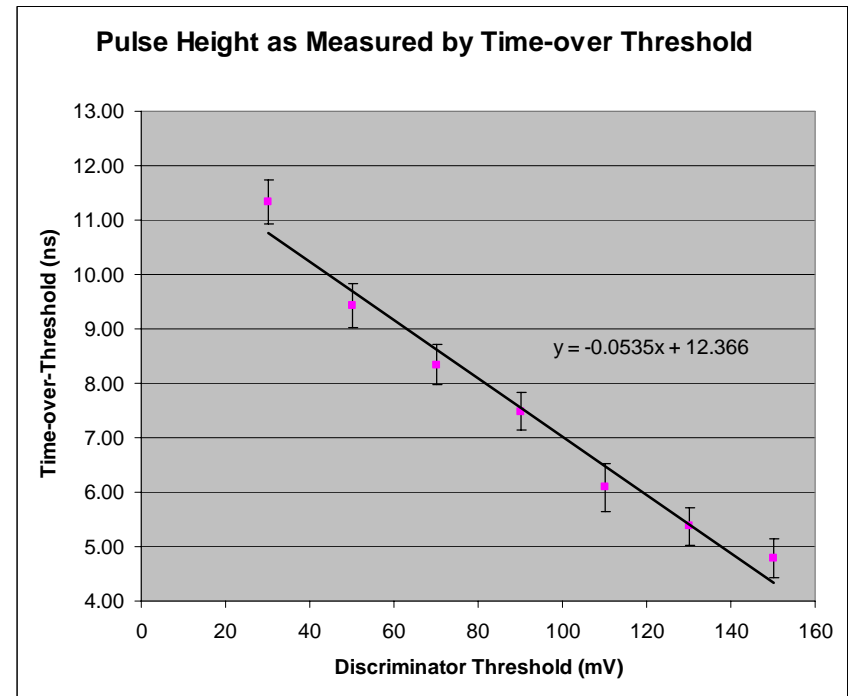
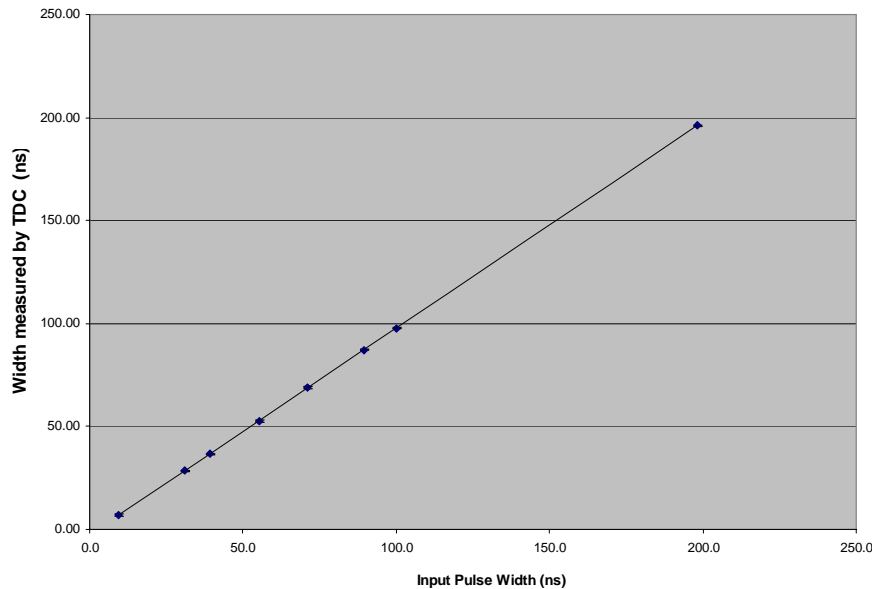
Two levels of noise caused by
number of helios entering the
channel. The first 32 are nearly 1 to 1
and the rest are close packed



Gains are stable

**Fit is to Mkn 421 background
which is low compared to the
Crab NSB**

Time Over Threshold Calibration



Average Pulse-width (100 samples) measurements on a 12 ns pulse as a function of discriminator threshold.

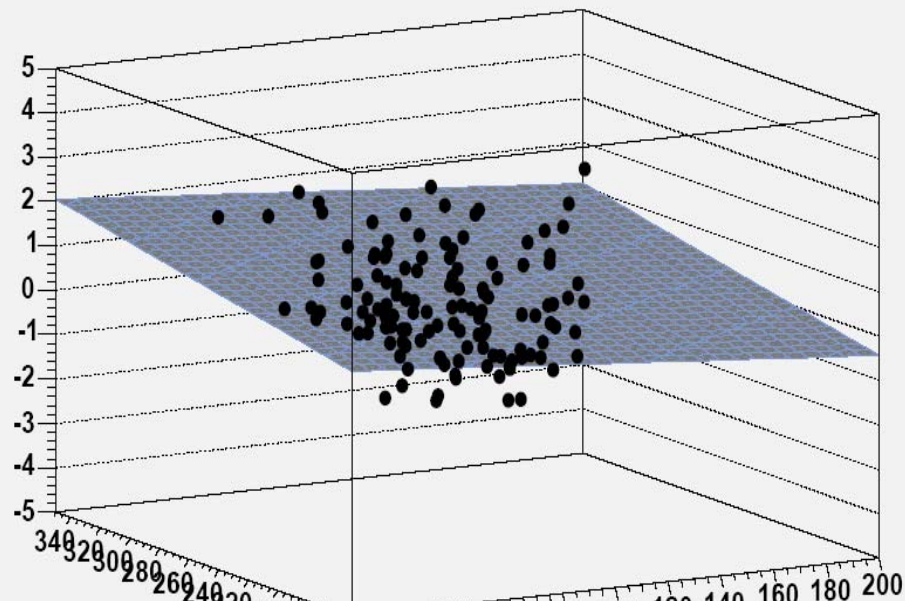
Effective resolution is
~50 ps/mV. Hence,

For a 0.5 ns TDC resolution on each edge an effective ToT resolution of ~0.7 ns is achieved.

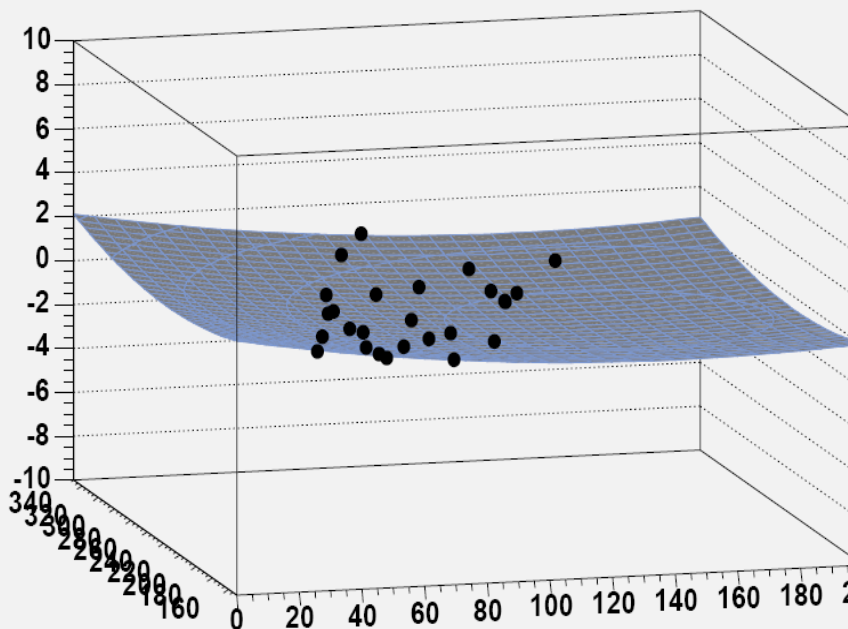
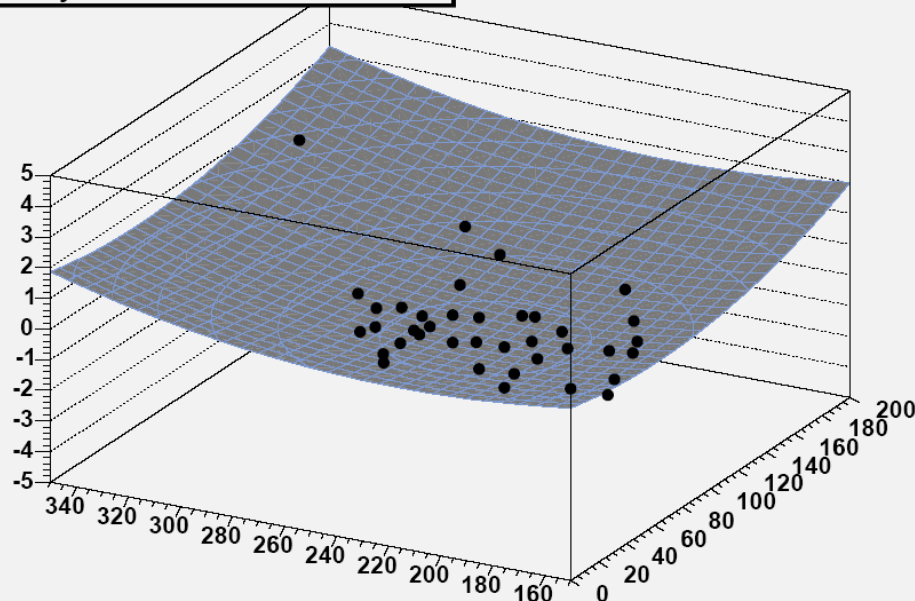
For a 1V dynamic range, this provides a 6-bit digitization.

Typical events with a
fitted wavefront
overlaid on the hits.

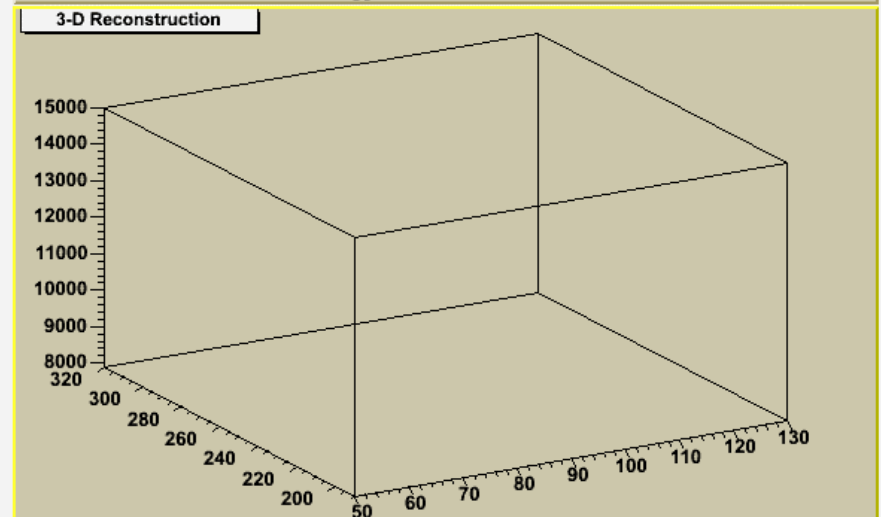
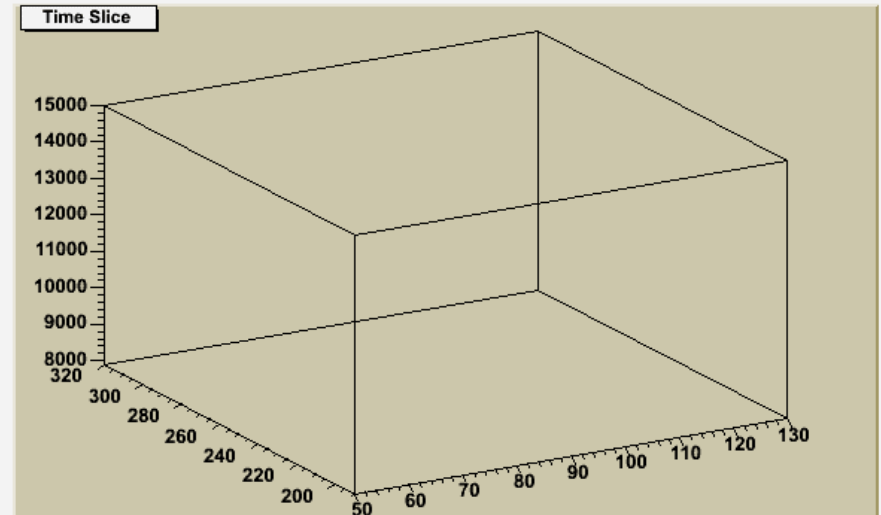
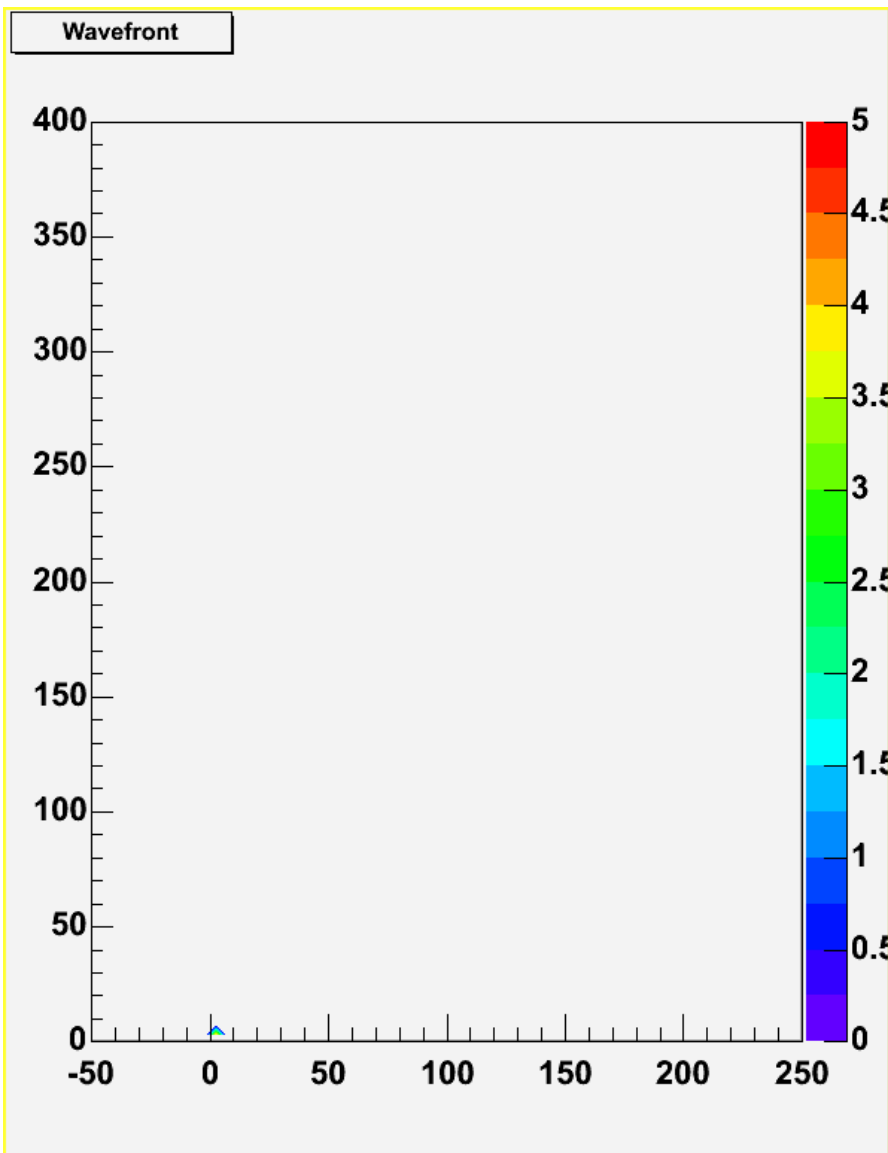
Overlay #Run9328 #Shower ID 113



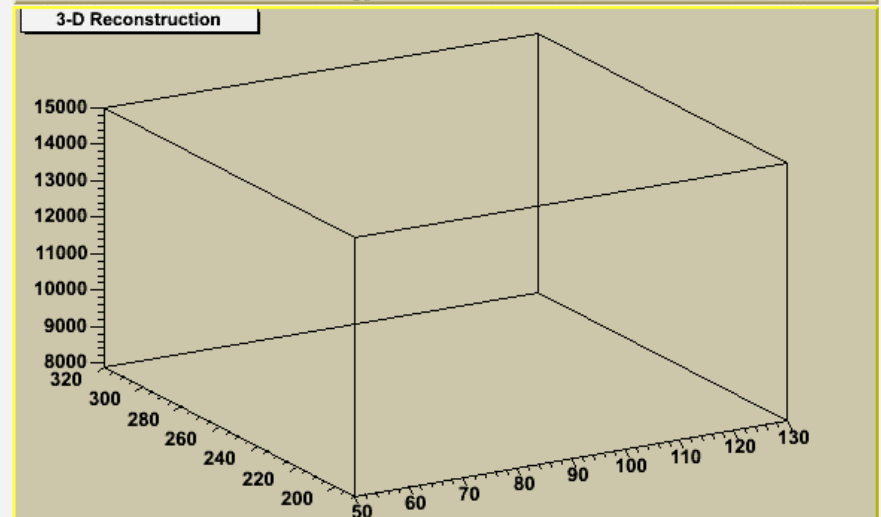
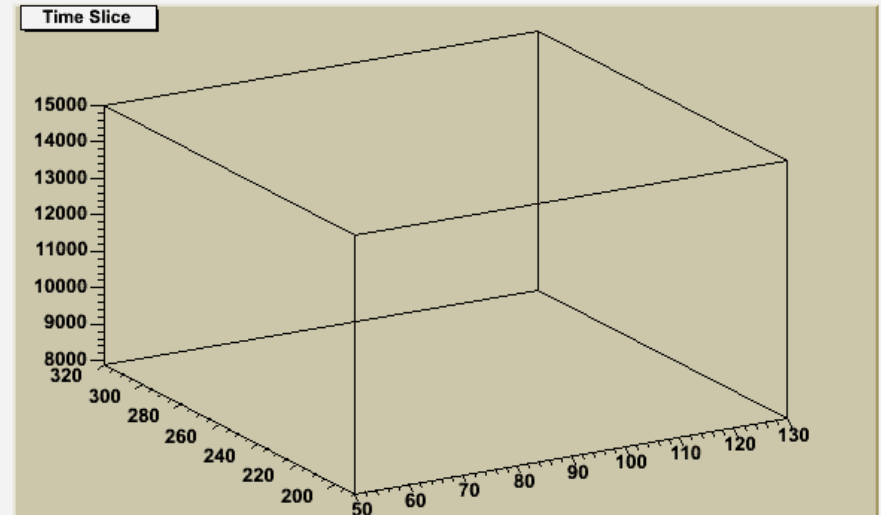
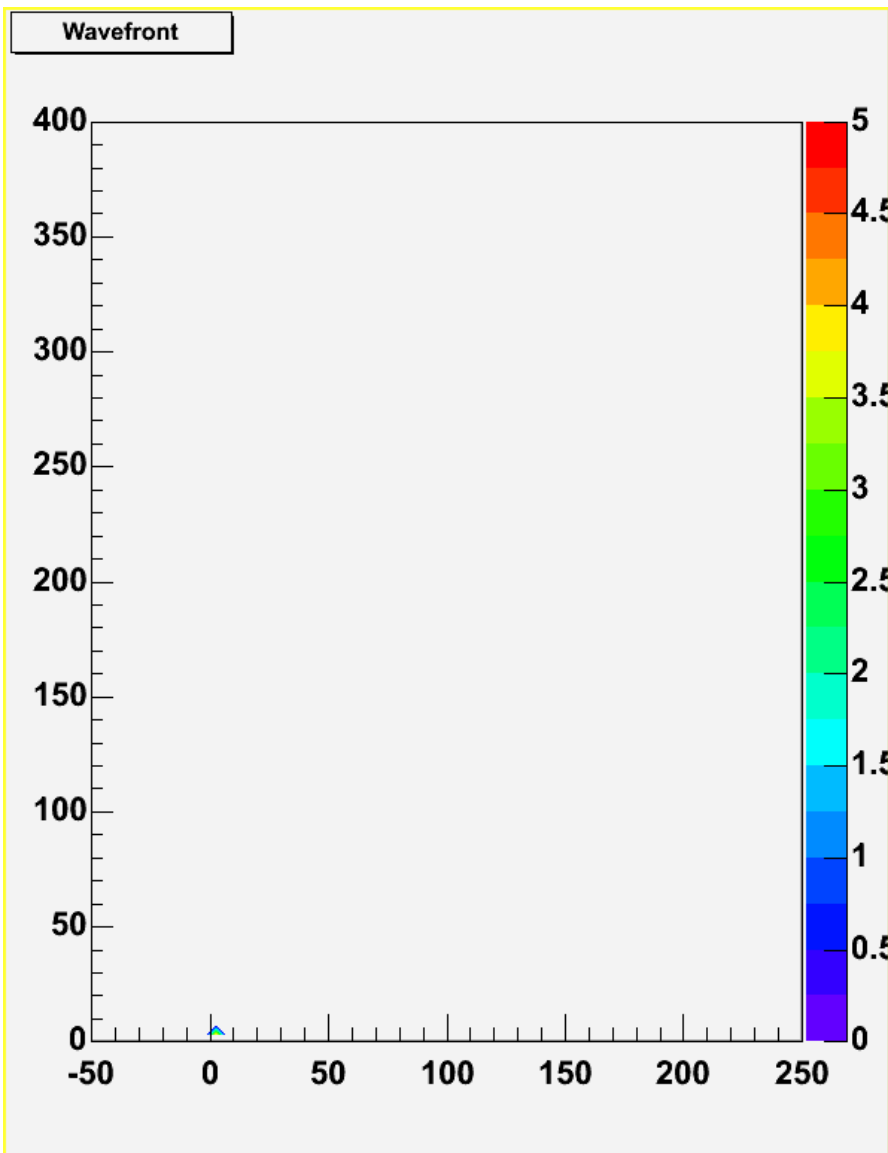
Overlay #Run9328 #Shower ID 261



Time Projection Reconstruction



Time Projection Reconstruction



Calibrations using the Crab Nebula

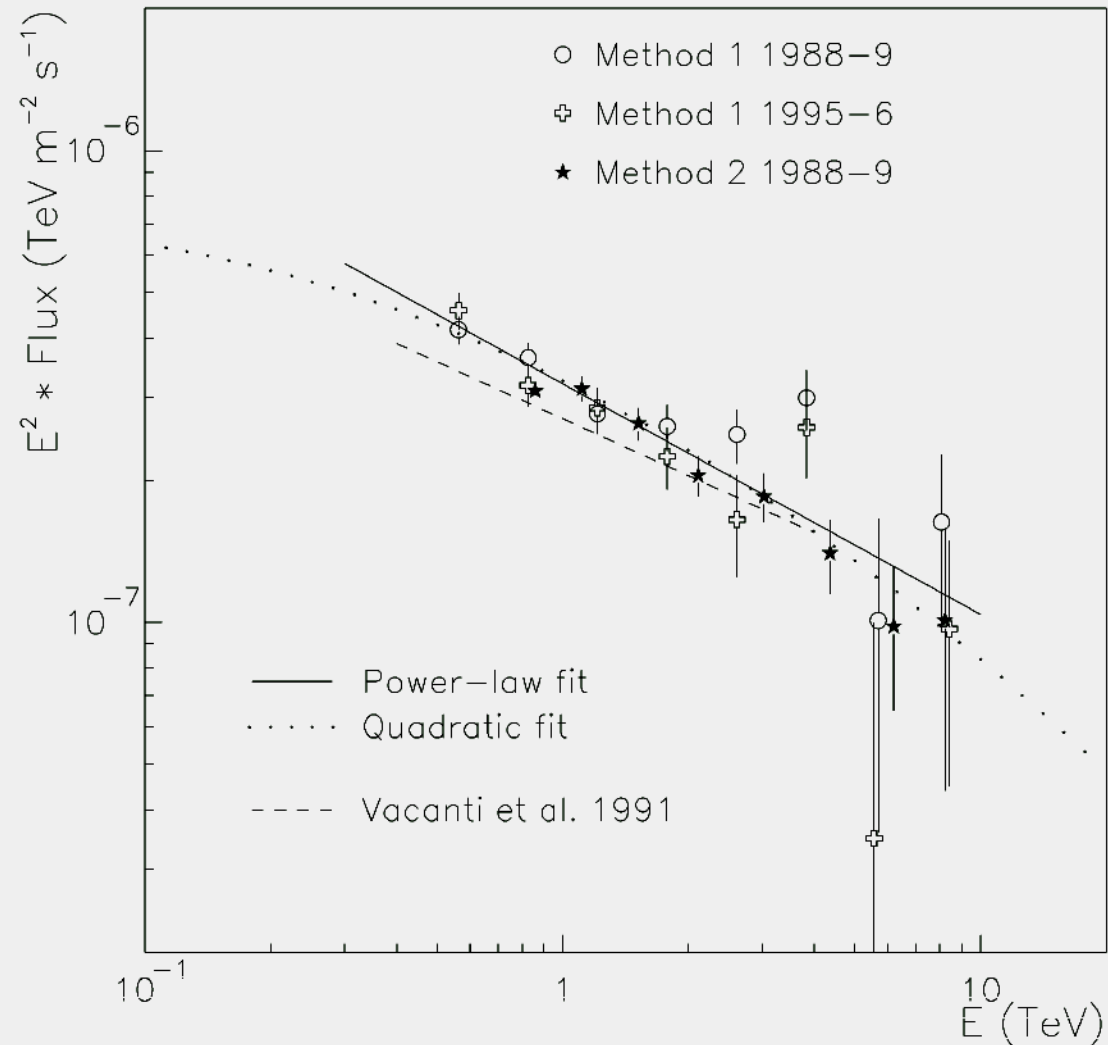
THE ASTROPHYSICAL JOURNAL, 503:744–759, 1998 August 20

The standard candle of gamma-ray astrophysics, the Crab has been studied extensively and is now believed to have a well known and stable spectrum above ~ 300 GeV.

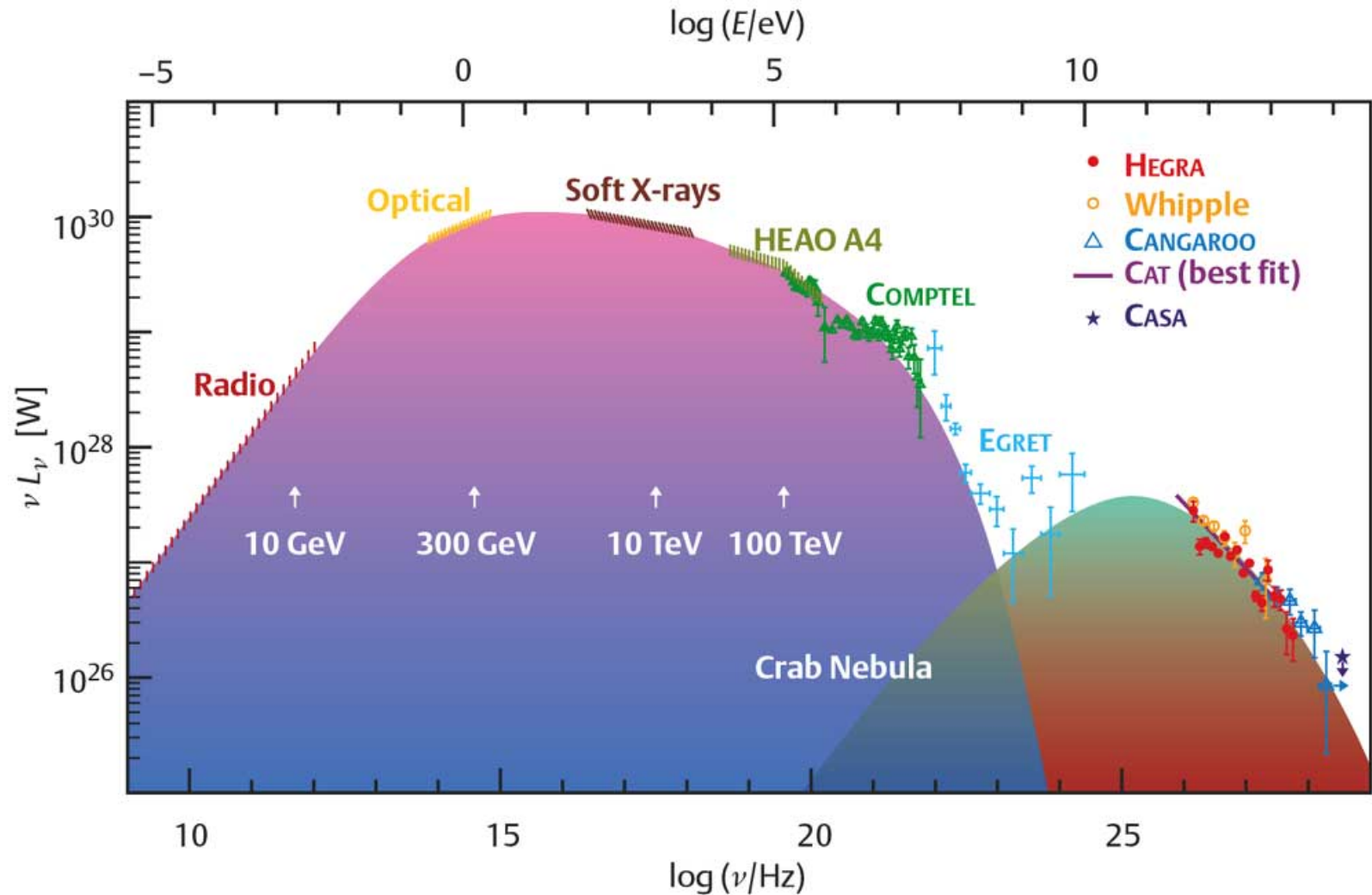


Mani Tripathi, UC-Davis

HILLAS ET AL.



Crab Spectrum: The spectrum has not been established in the 10-100 GeV region, thus making it difficult to use the Crab as a standard candle in this regime. We have to rely on simulations.

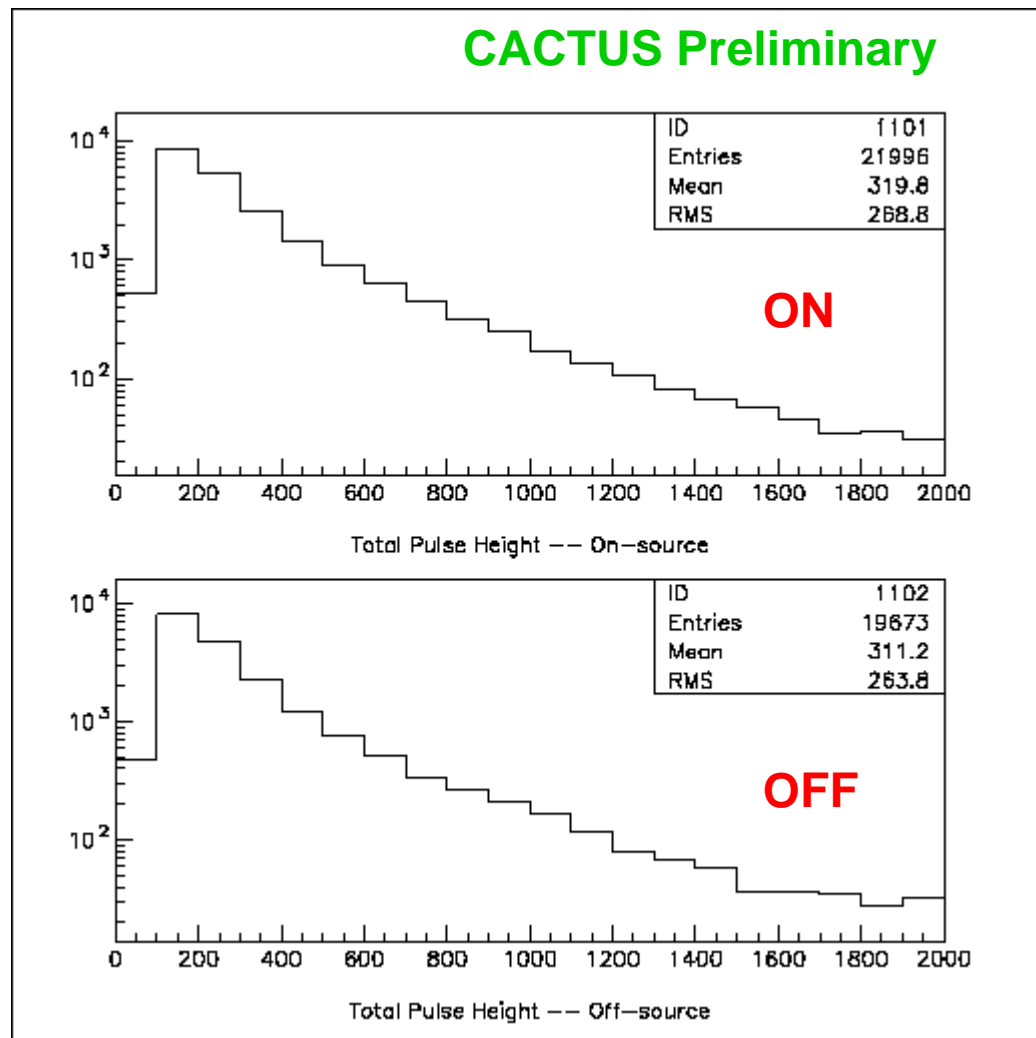


CRAB: The observed distribution in Total Pulse-Height.

Data are recorded in ON-source (heliostats track the Crab) and OFF-source (heliostats revert and track a point 30 mins away from the Crab) pairs of 28 minute duration each.

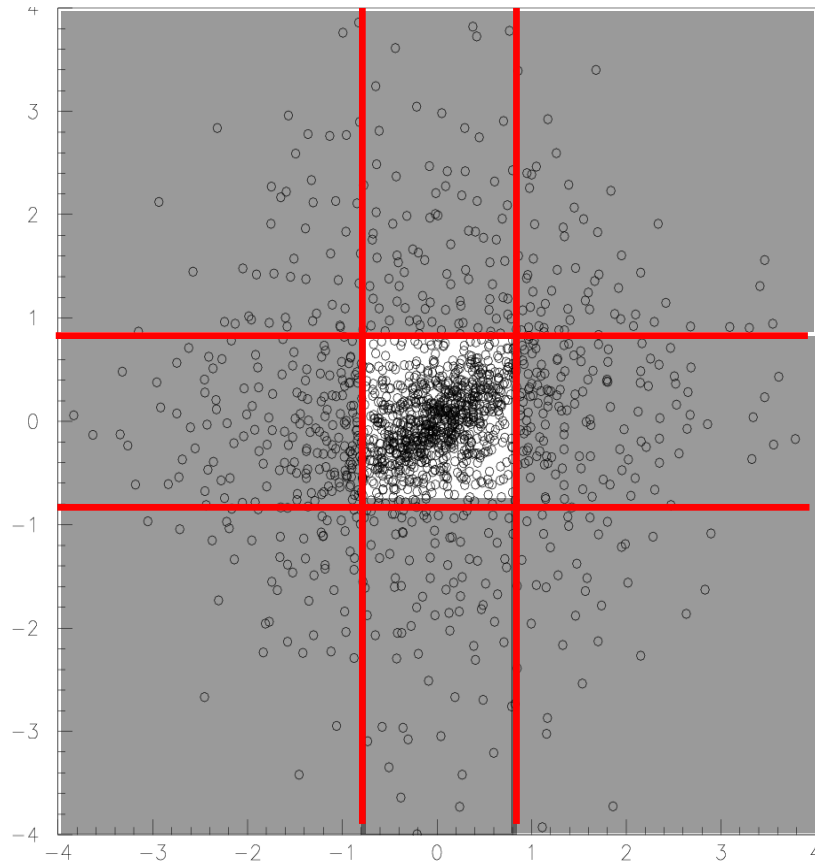
We require >20 channels in a 13 ns window for the event to be considered in our offline sample.

Further fiducial cuts are applied on the measured centroid and angle to restrict the sample to well contained events (next slide).



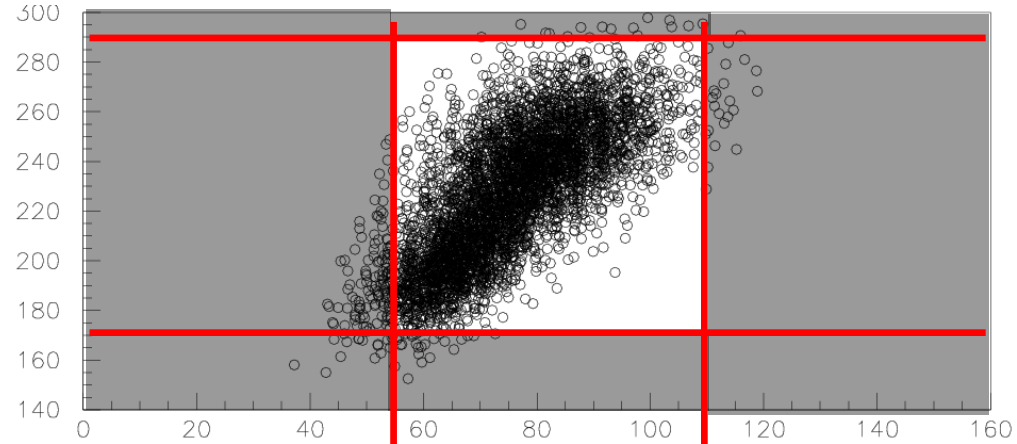
Fiducial Cuts

First Planar Angle Fit

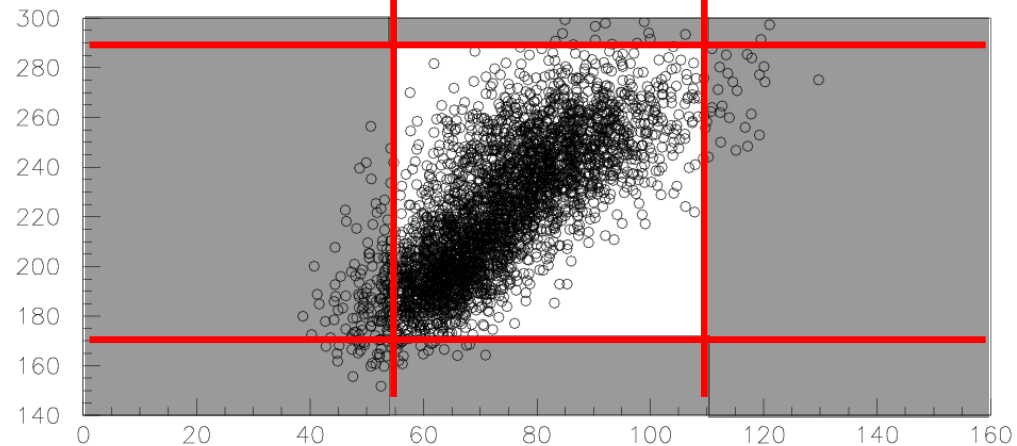


Y ang vs X ang -- Triggered -- On-Source

X/Y Shower Centroids



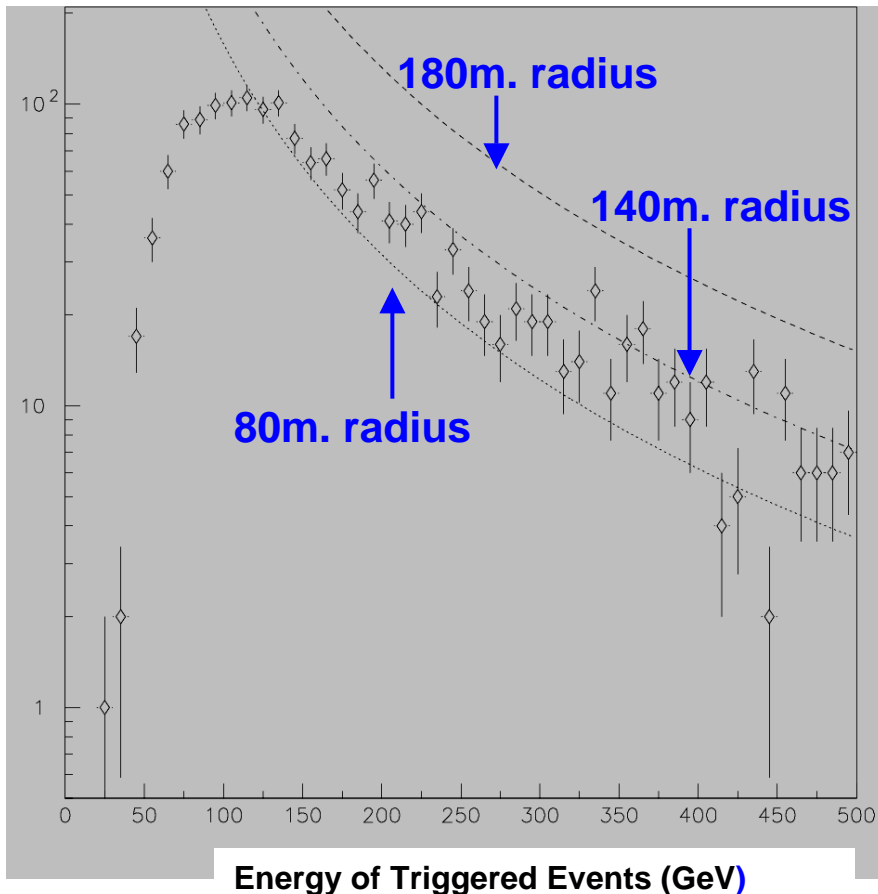
Centroid -- Triggered -- On-Source



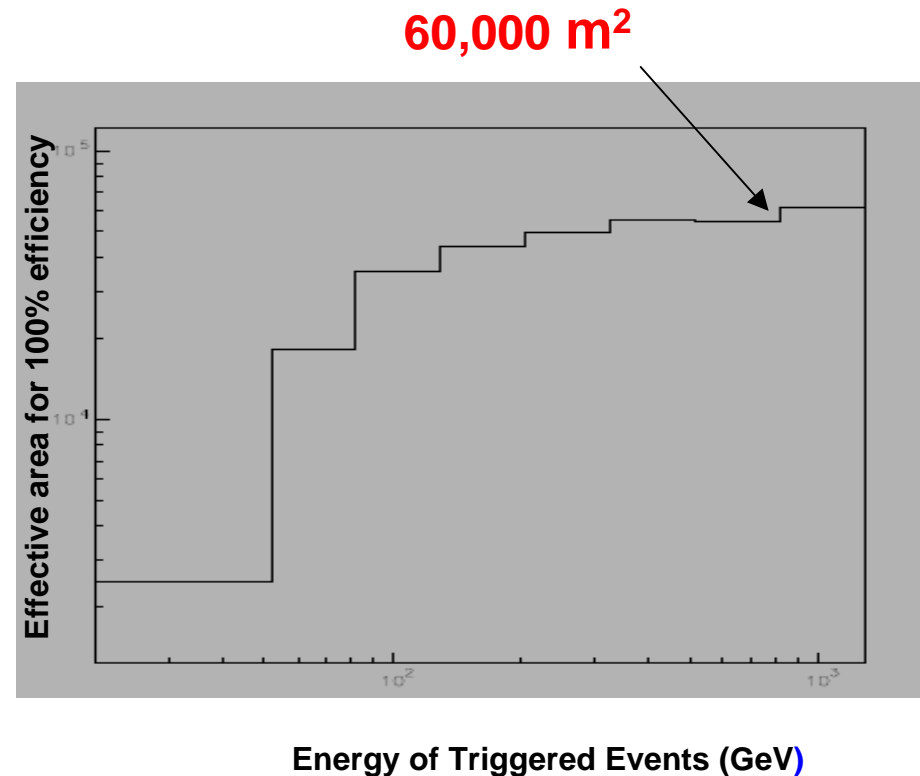
Centroid -- Triggered -- Off-Source

Efficiency and Effective Area

Input spectrum = $k \cdot E^{-2.4}$



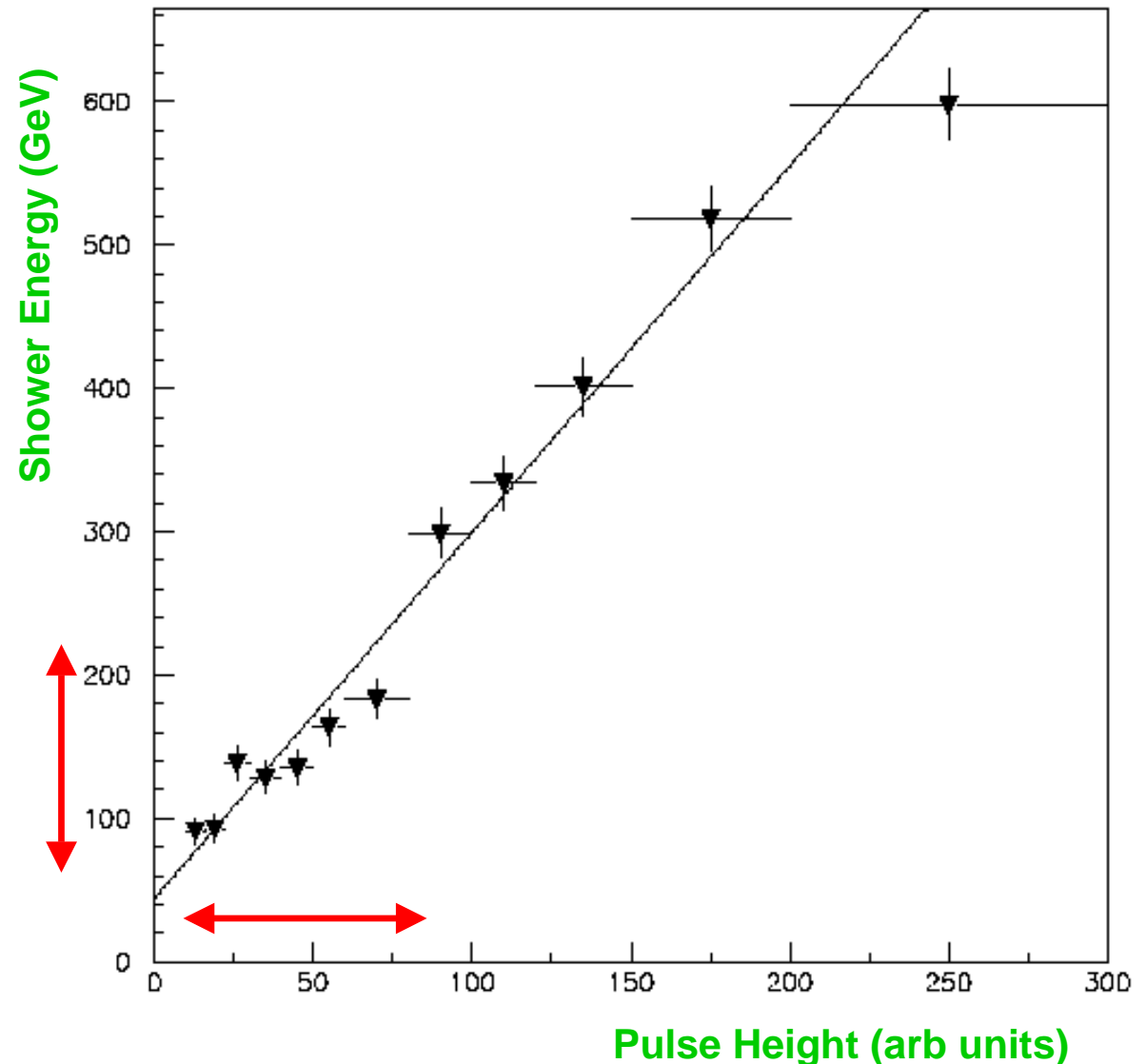
Simulations indicate an effective area of ~140m radius for energy > 500 GeV.



Preliminary analysis of pulse-height and energy calibration from simulations.

This is a difficult region to calibrate because we rely on the Crab spectrum. However, Crab spectrum below 100 GeV is not known.

More detailed simulations are in progress.

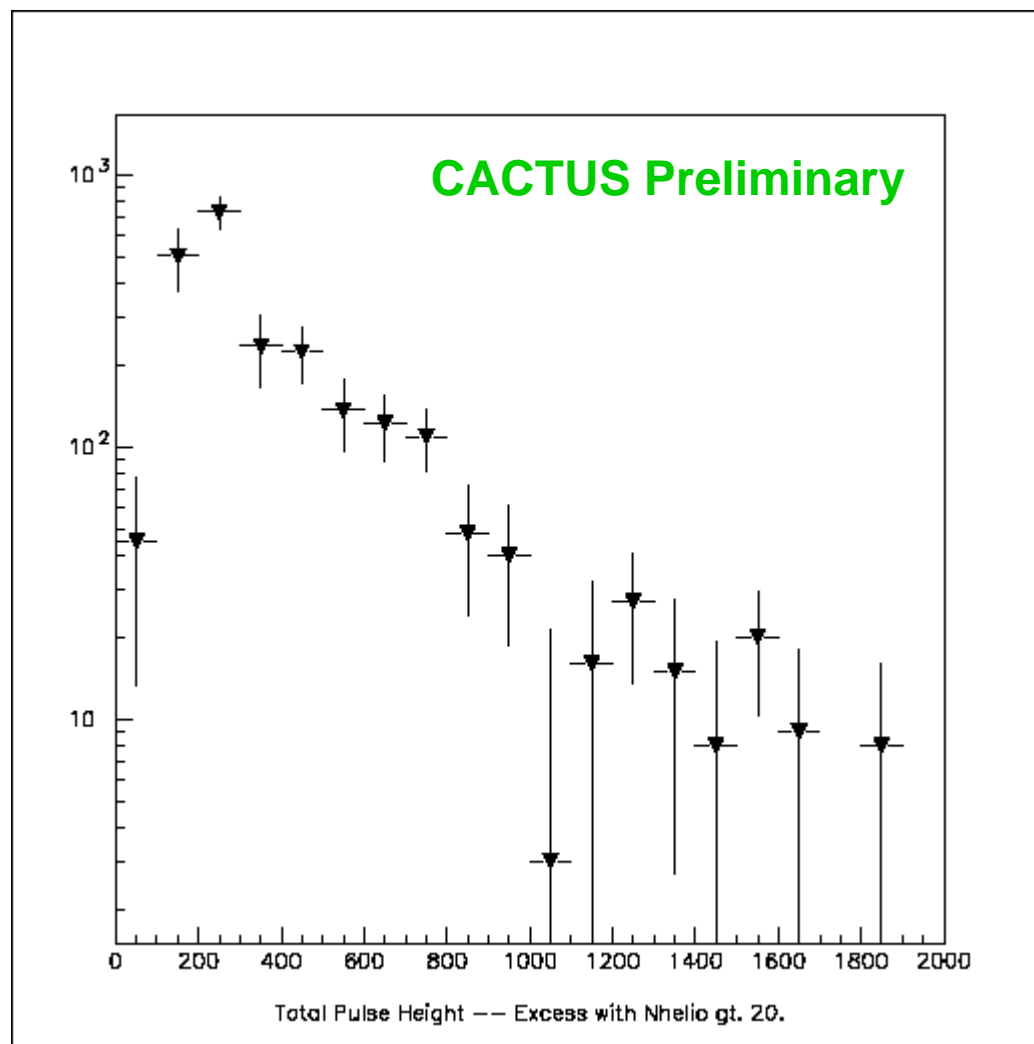


CRAB: Measured excess for “high energy” events

This sample from the Crab represents an excess rate of **12/min.**

The horizontal scale is “total measured pulse height” which is closely related to the incoming energy.

The range of measurements here represent an energy range of ~ 50-2000 GeV.



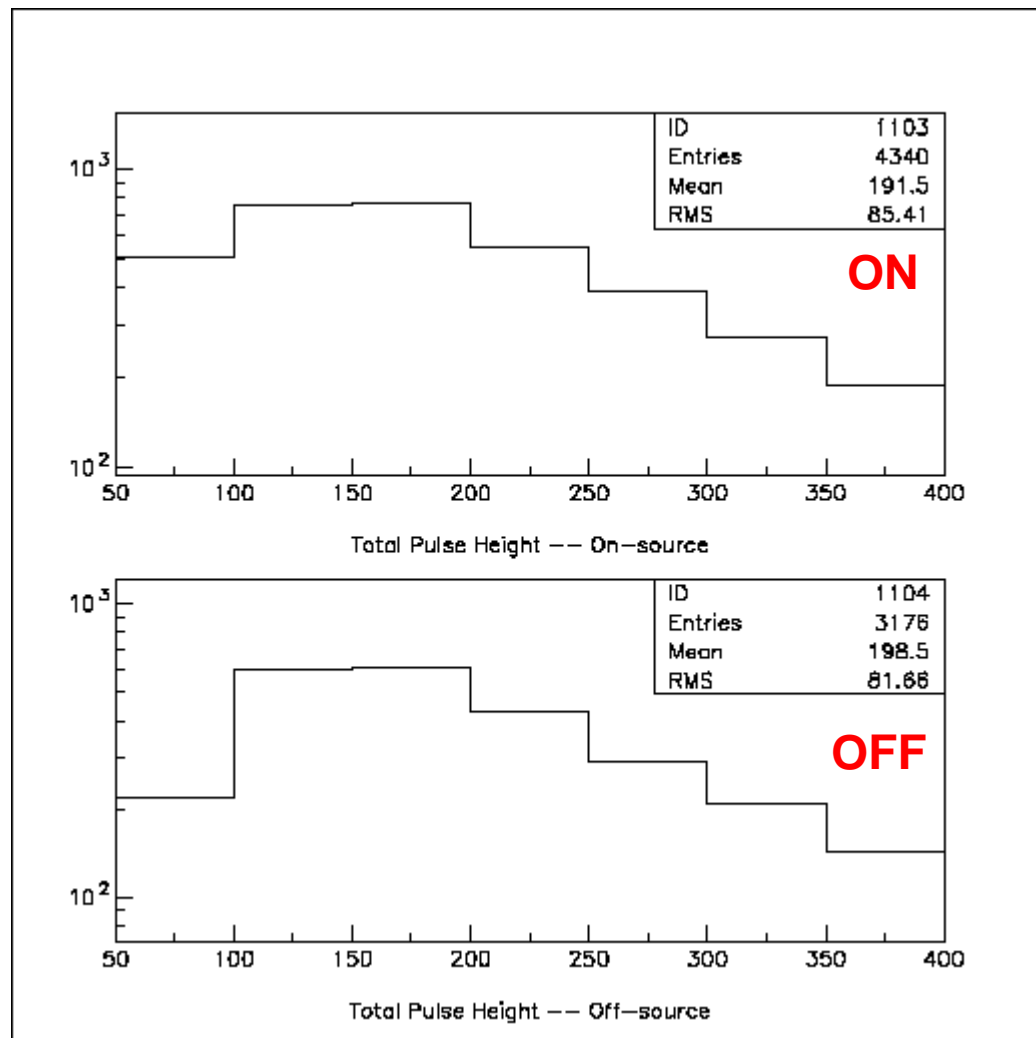
CRAB: Attempt at understanding the low energy regime

Lower the requirement for Number of channels in the trigger (>15).

Same fiducial cuts as before.

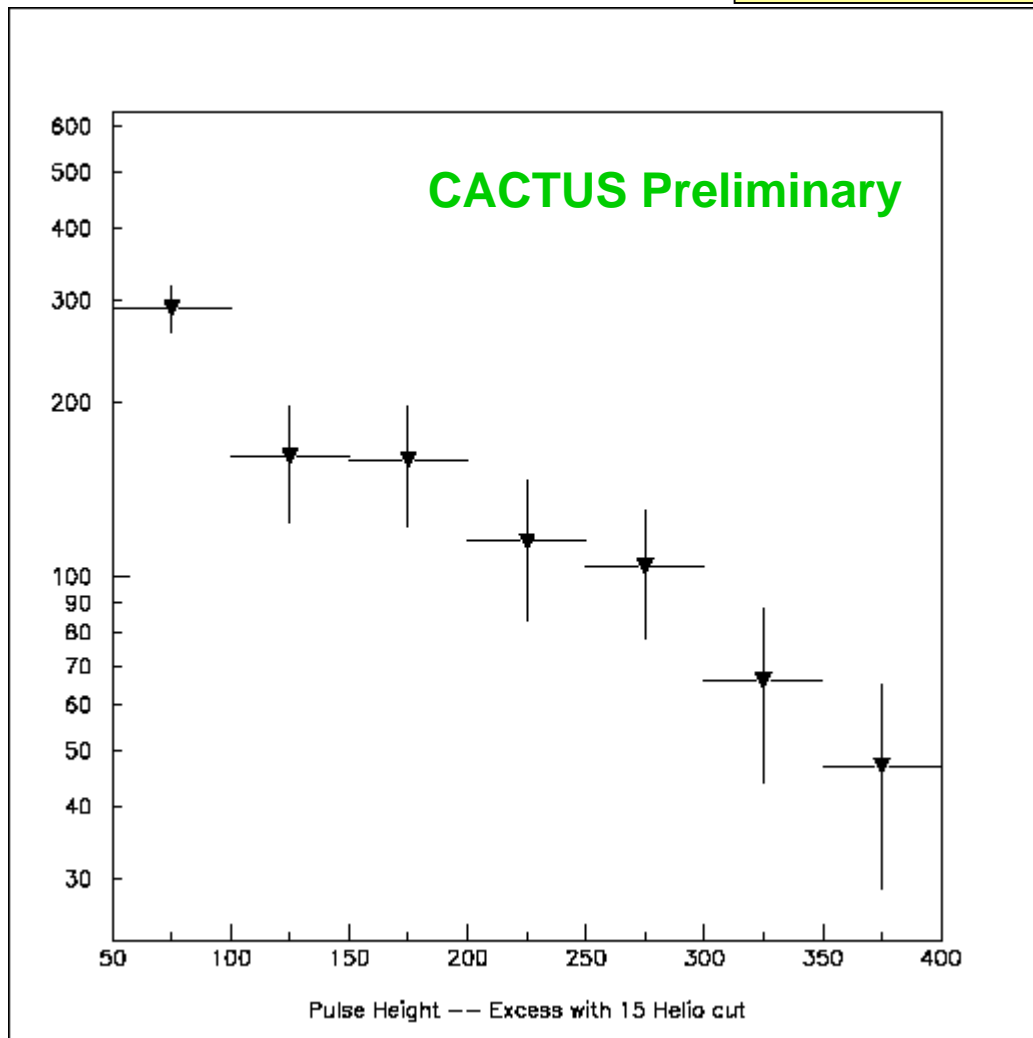
Restrict the data set to one on/off pair (28 mins) to avoid weather related differences.

Observed excess of events after cuts = **42/min**.



CRAB: Measured excess for “low energy” events

Crab low energy excess: Rate of ~ 42/min!



The significance of this detection of Crab in 28 mins is 13σ .

Much work remains to be done before a final flux measurement can be extracted.

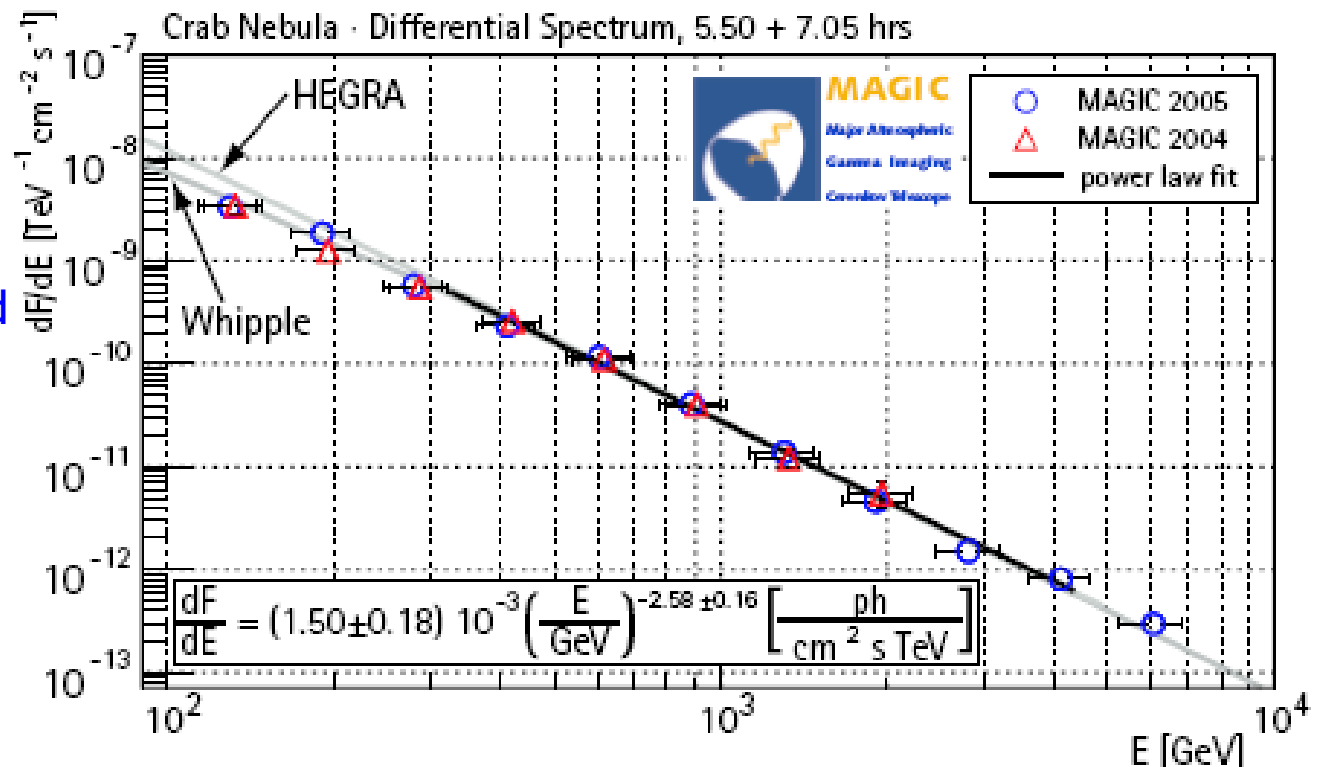
Recent Measurements of the Crab

29th International Cosmic Ray Conference Pune (2005) **00**, 101–106

Observations of the Crab nebula with the MAGIC telescope

R. M. Wagner^a, M. Lopez^b, K. Mase^{a,f}, E. Domingo–Santamaria^c, F. Goebel^a, J. Flix^c, P. Majumdar^a, D. Mazin^b, A. Moralejo^d, D. Paneque^a, J. Rico^c, and T. Schweizer^e
on behalf of the MAGIC collaboration

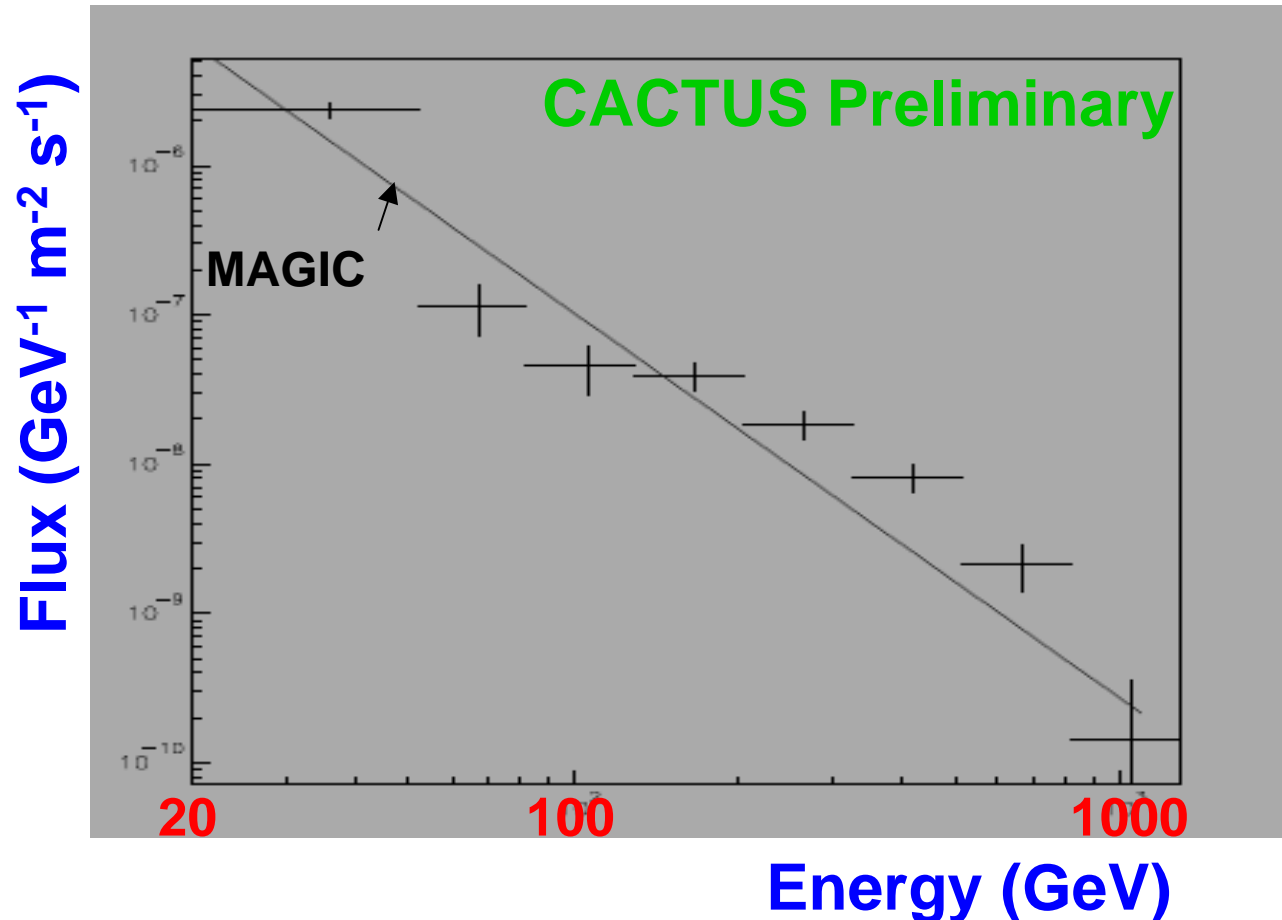
The lowest data point is at ~130 GeV with a flux of $\sim 5 \times 10^{-8} \text{ GeV}^{-1} \text{ m}^{-2} \text{ s}^{-1}$. This is a good calibration point.



CACTUS Measurement of the Crab Spectrum

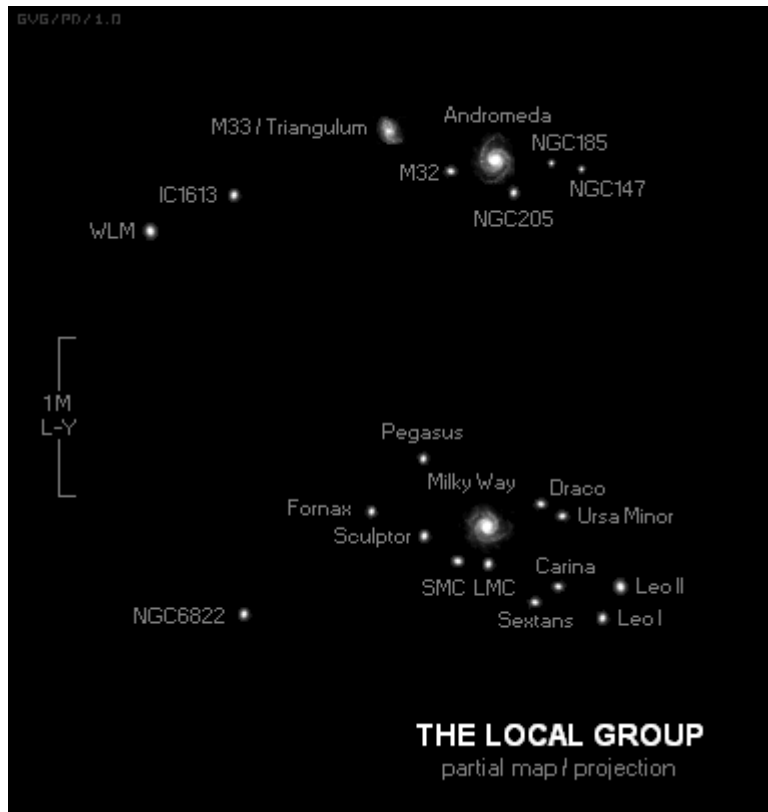
Using a shower wavefront fitting technique, we are able to improve our energy resolution, albeit with some loss in efficiency.

Our measured Flux at low energies seem to be in agreement with an extrapolation of the MAGIC fit.



Draco and Dark Matter

Draco is a dwarf spheroidal galaxy in the vicinity of the Milky Way. Its estimated total mass of is $\sim 0.3 - 8 \times 10^7$ solar masses and, given the low luminosity of $\sim 2 \times 10^5 L_{\text{solar}}$, the global mass-to-light ratio anywhere in the 10-100 range. This requires that Draco contain a dominant dark matter component.



Draco is about 0.5 degrees across. It is very faint in the optical.

Integrated magnitude ~ 11 making it an ideal candidate for ACT observations.



Neutralinos: Previous attempts at understanding Draco.

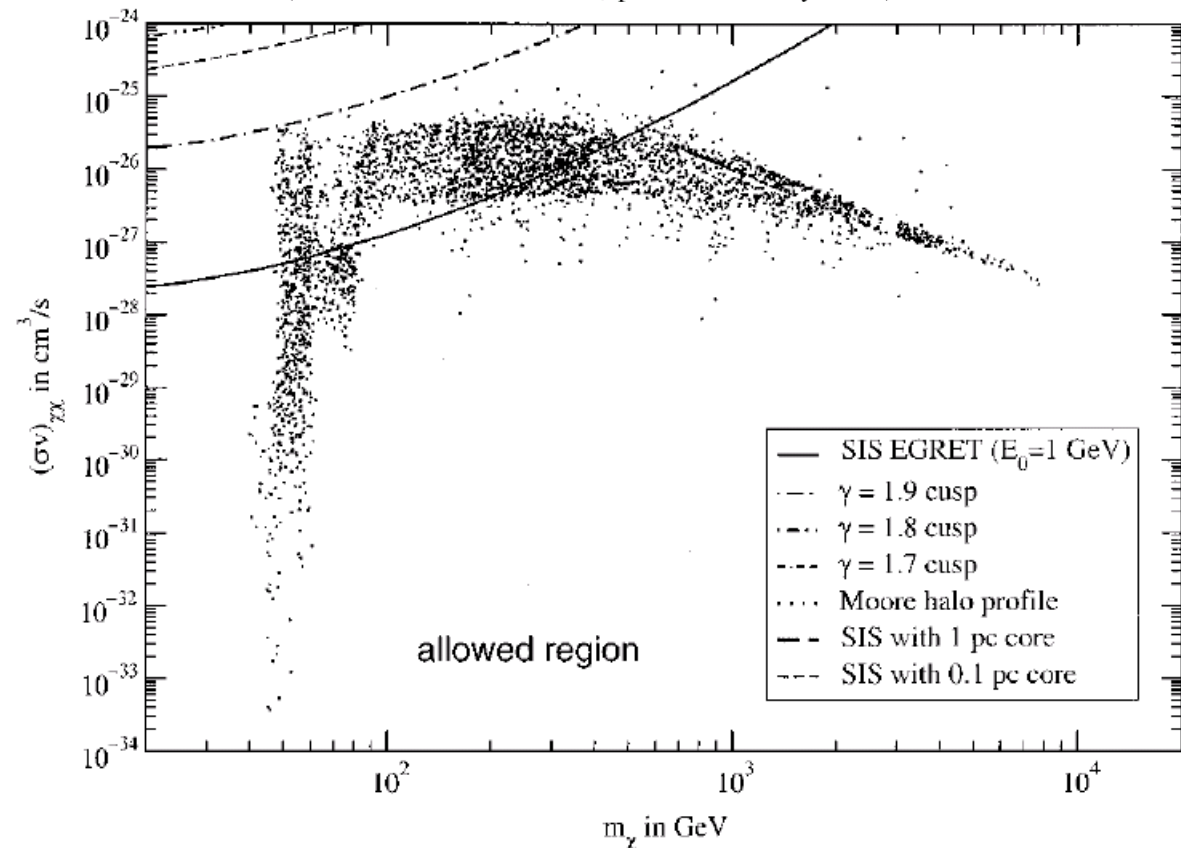
PHYSICAL REVIEW D **66**, 023509 (2002)

Particle dark matter constraints from the Draco dwarf galaxy

Craig Tyler*

Department of Astronomy & Astrophysics, The University of Chicago, Chicago, Illinois 60637

(Received 18 March 2002; published 3 July 2002)



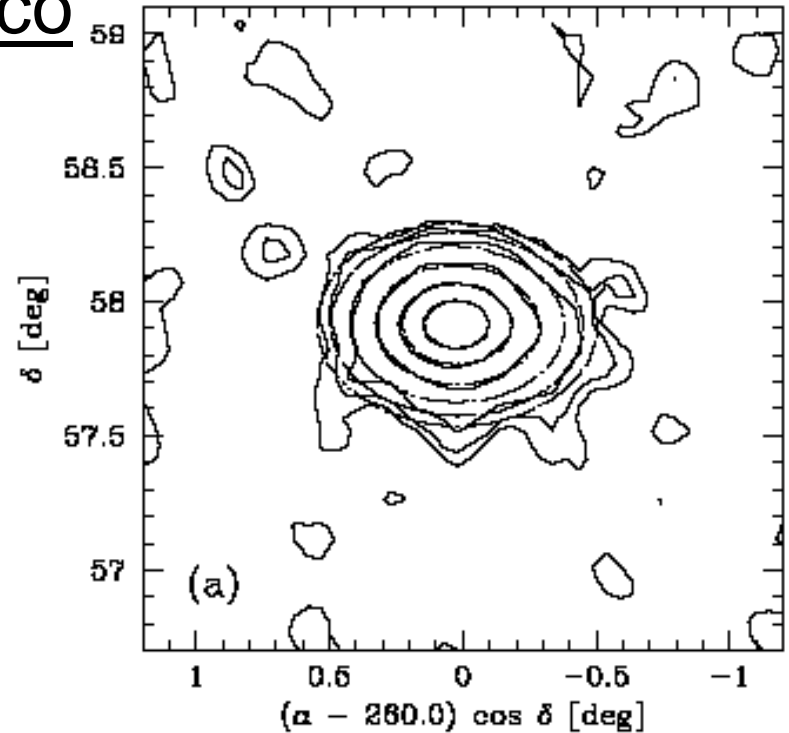
Neutralinos are the lowest mass supersymmetric particles in the Minimum SUSY Model. Since they are stable, they are a popular candidate for Cold Dark Matter.

Neutralinos can annihilate into quark and anti-quark pairs. The resulting hadron jets will contain gammas from neutral pion decays.

The rate will depend on ρ^2 , where $\rho \sim r^{-\gamma}$ is the density profile of the neutralinos.

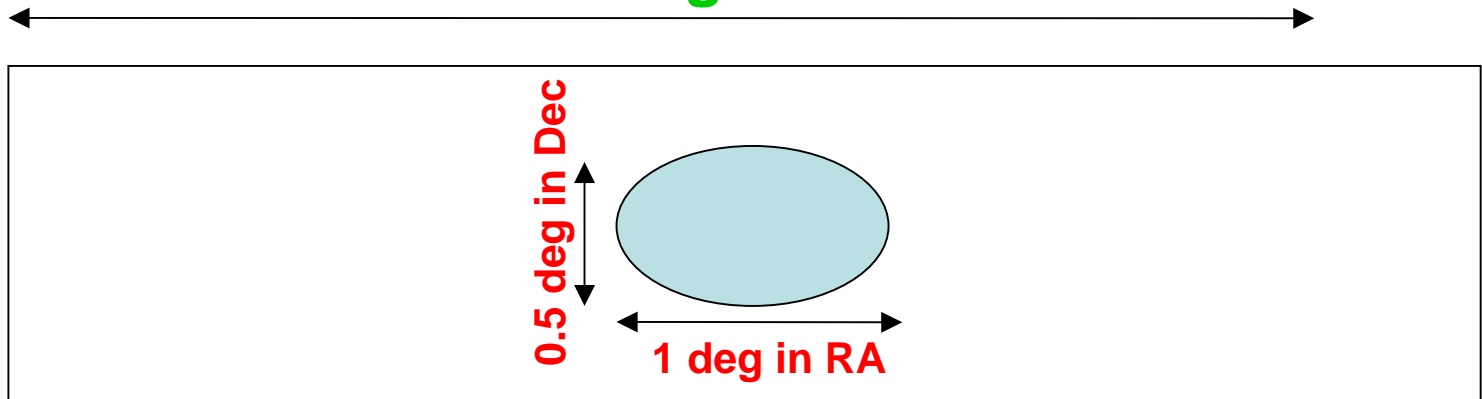
CACTUS Observations of Draco

SDSS map



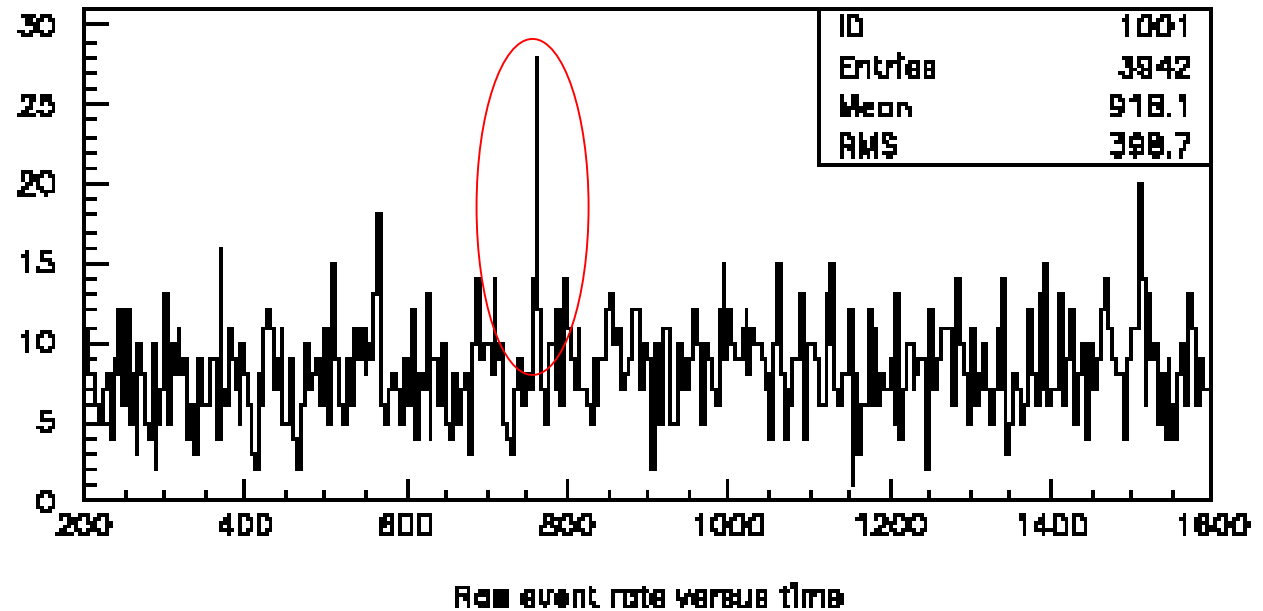
4 degrees in RA

~1 deg in Dec

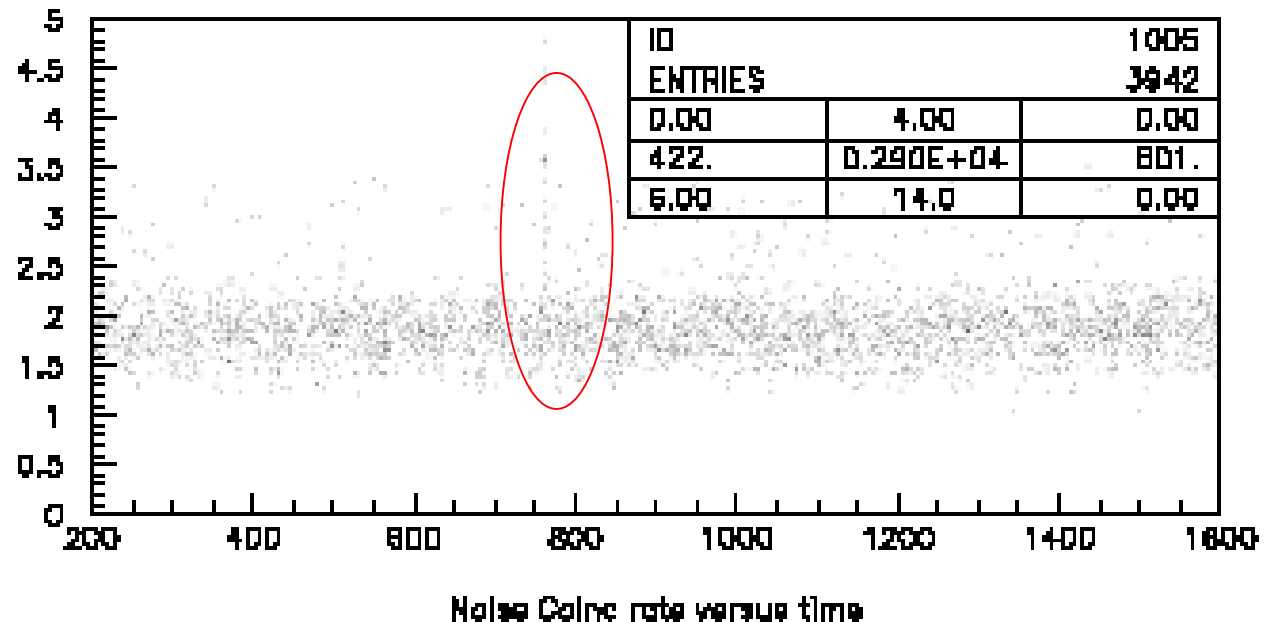


Typical Scan lasting 30 minutes

The data-acquisition consists of recording time of arrival and pulse heights for each channel. In addition, background noise rates are recorded for 1 microsecond preceding the triggering event.



Noise spikes due to fluctuations and/or meteorites, airplanes etc can be tracked in the background noise rate which is otherwise very stable.

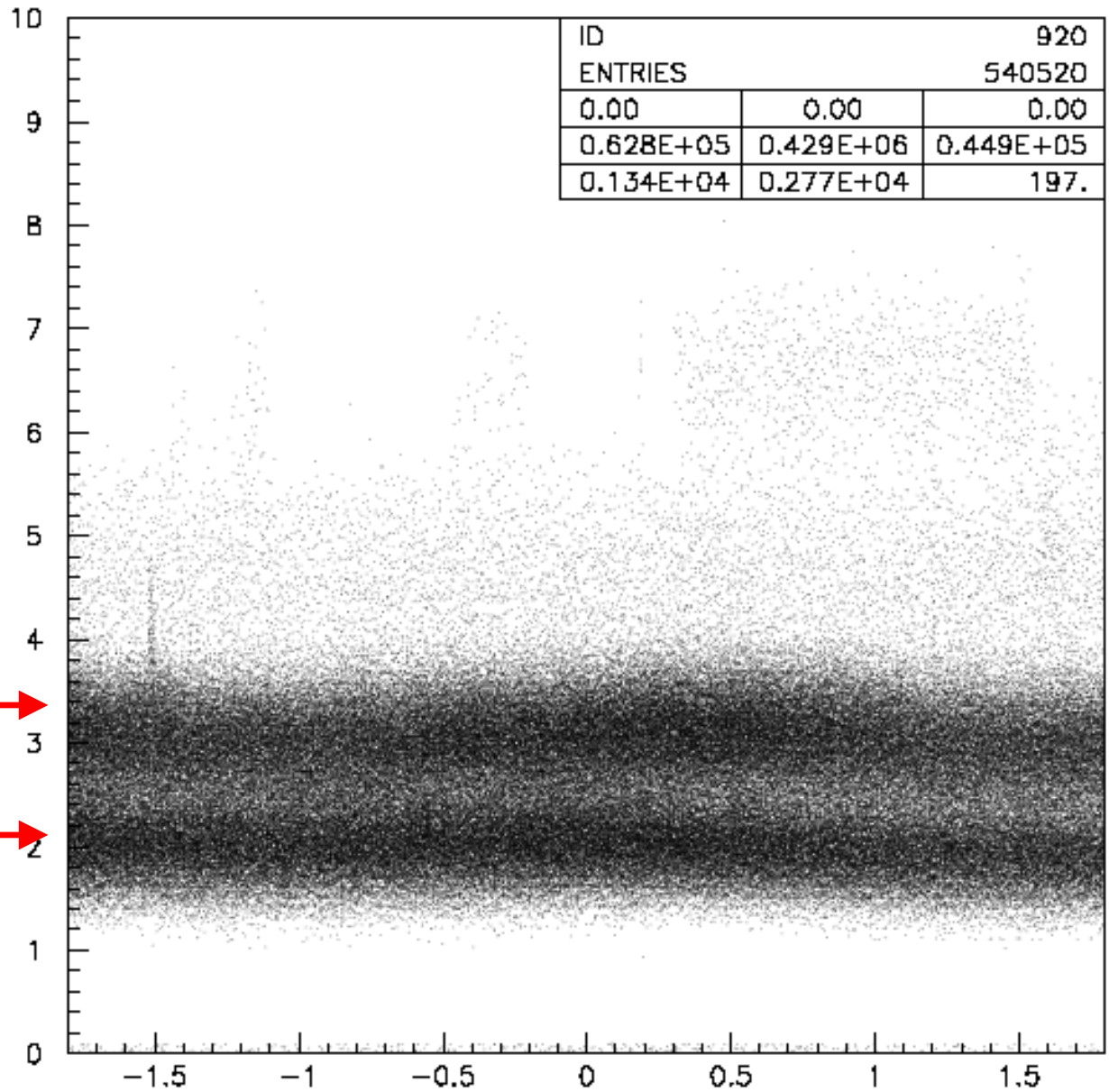


Integral of 44 scans

During the 10 days of observing the night sky had a small shift in transparency. The noise coincidence rate went up and the trigger was adjusted to accommodate this change.

Trigger on >13
channel coincidence →

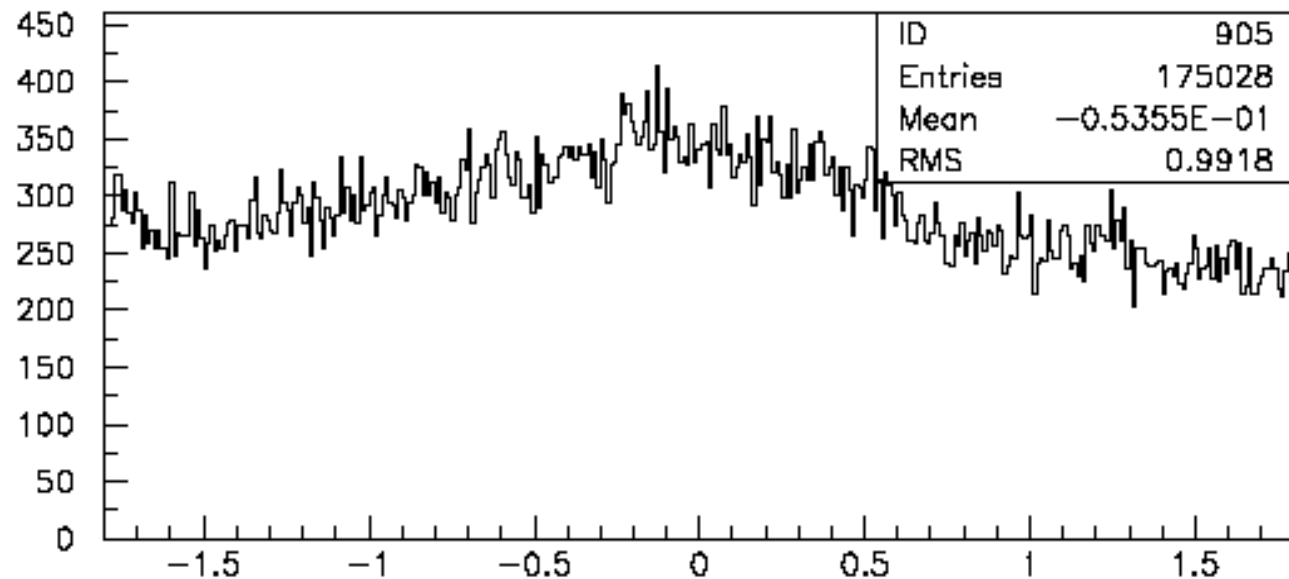
Trigger on >11
channel coincidence →



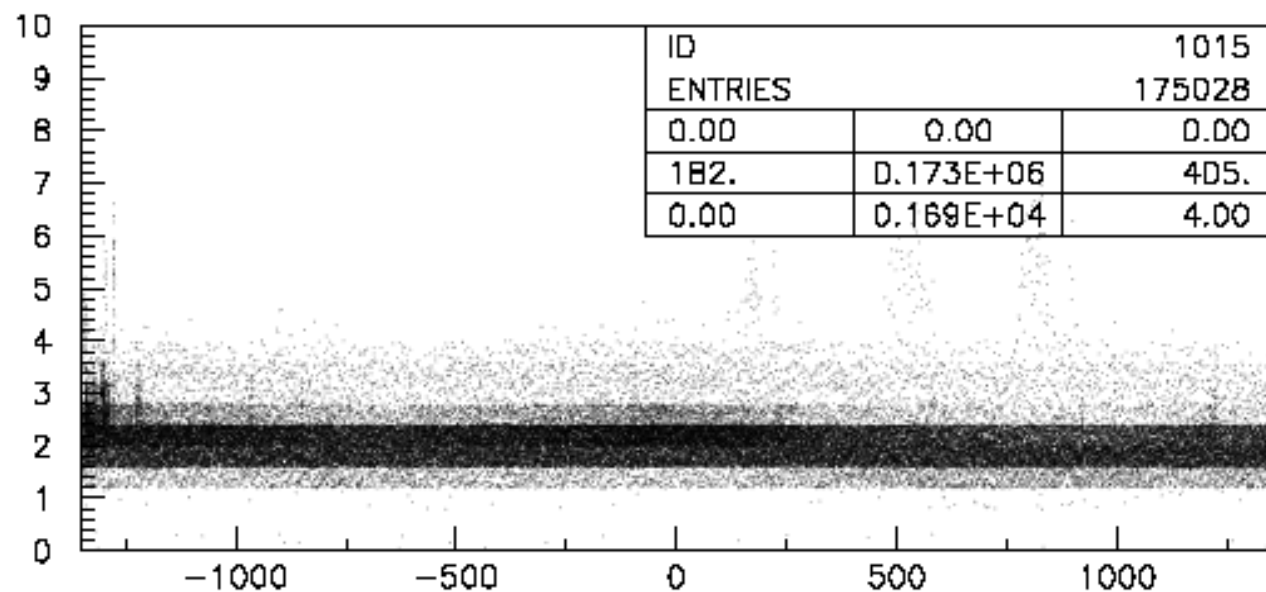
Raw Noise Coincidence versus RA — 0.01 degree bins

Sum of 7 scans
taken during low
background rate
conditions.

The background
is stable, while
the scan data
show a feature.



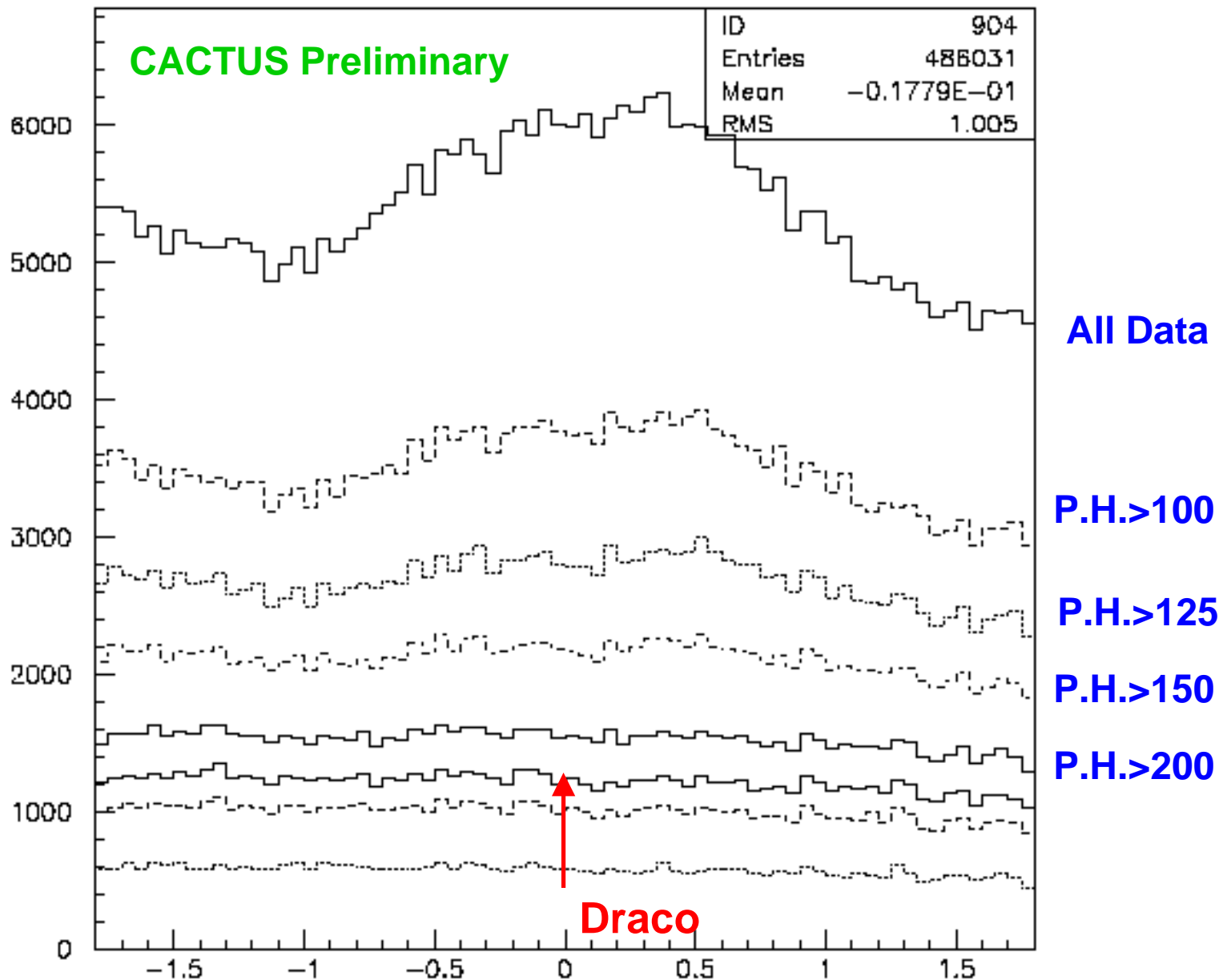
Raw events versus RA — 0.01 degree bins



Raw Noise Coincidence rate per 4s versus time

Integral of 44 scans

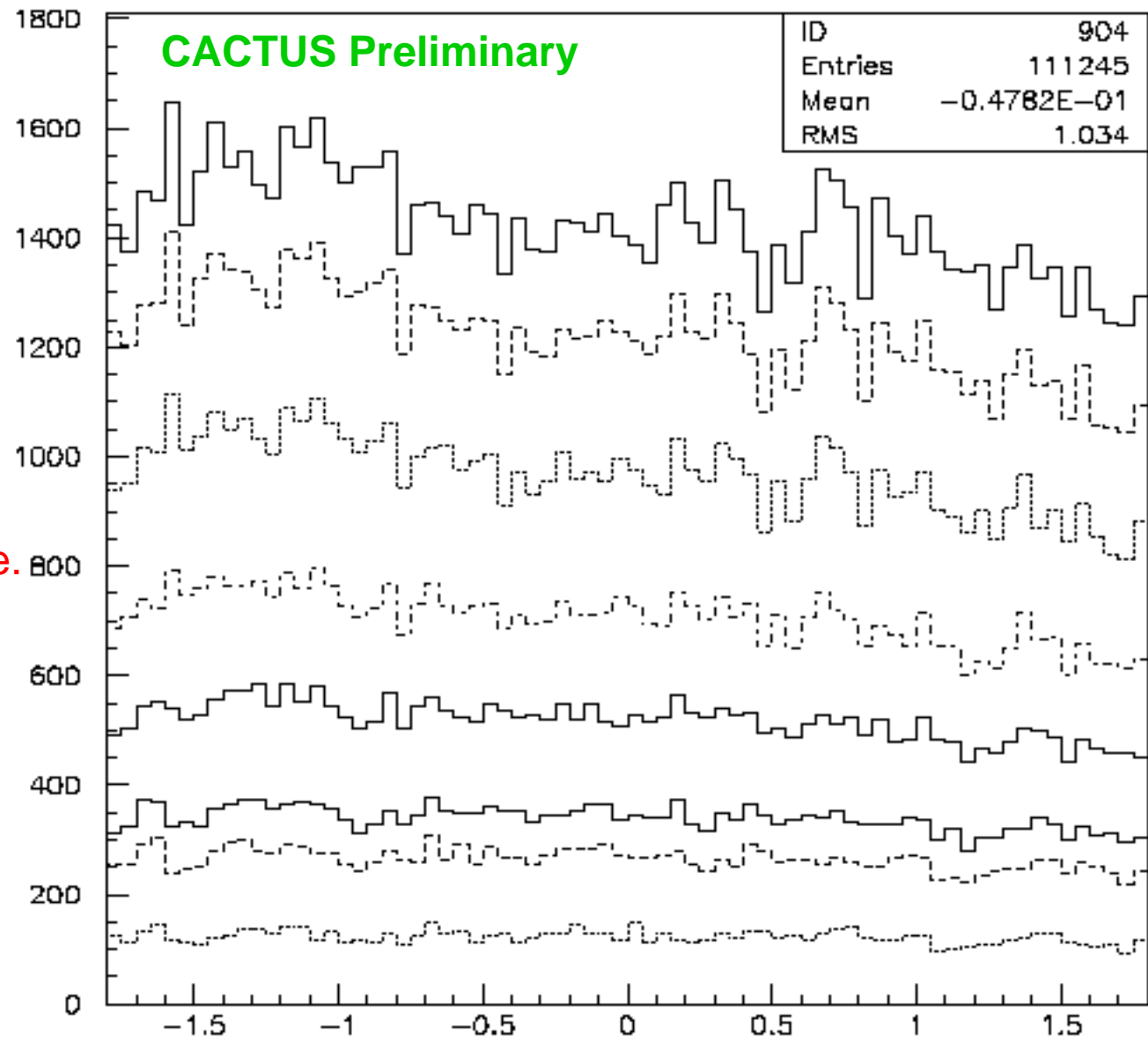
Placing cuts
on the total
Pulse Height
in the event
(~energy)
reveals that
the excess
is not visible
above about
150, which is
~150 GeV.



Scan of Draco -1 in Dec

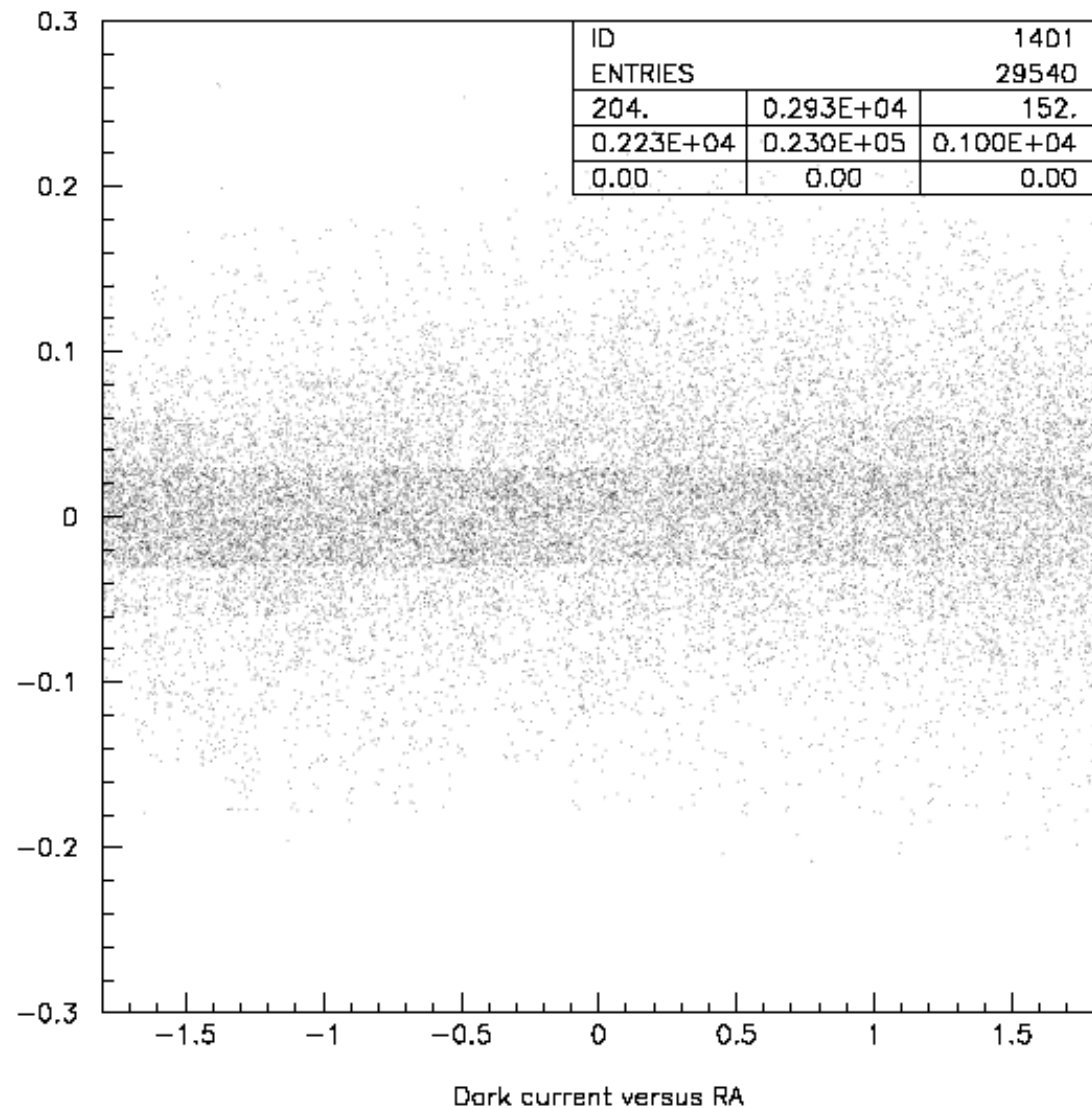
A similar set of scans in RA but offset by 1 degree in Dec show flat distributions in all energy bins.

A total of 10 scans are integrated here. The scaled rates agree with the background in 44 Draco scans.



Dark Currents
were also quite
stable for the
duration of the
scans.

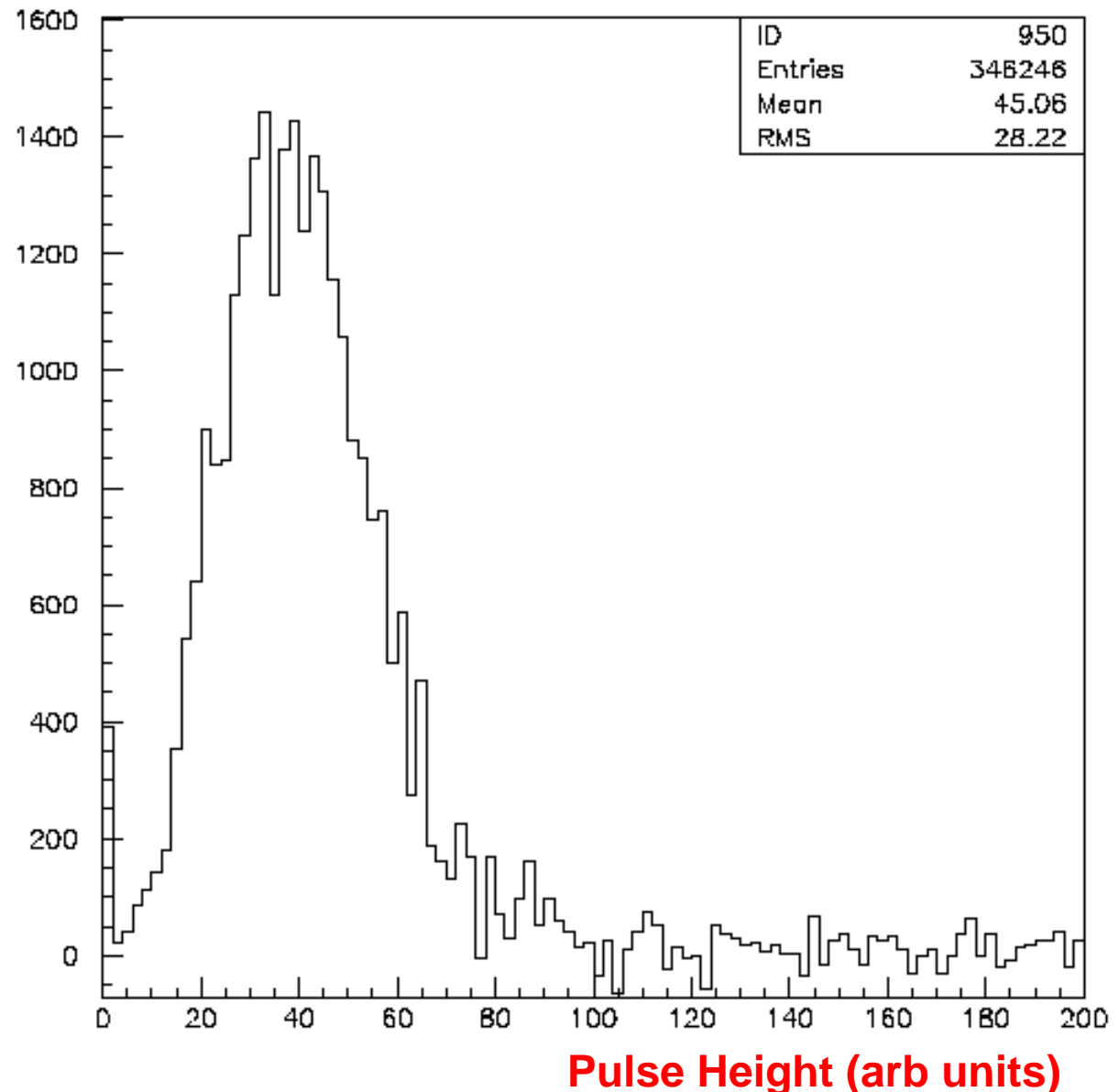
Shown here is
the deviation
from the
baseline
average dark
currents
recorded during
1 minute prior
to the scan.



Energy Distribution of the Excess

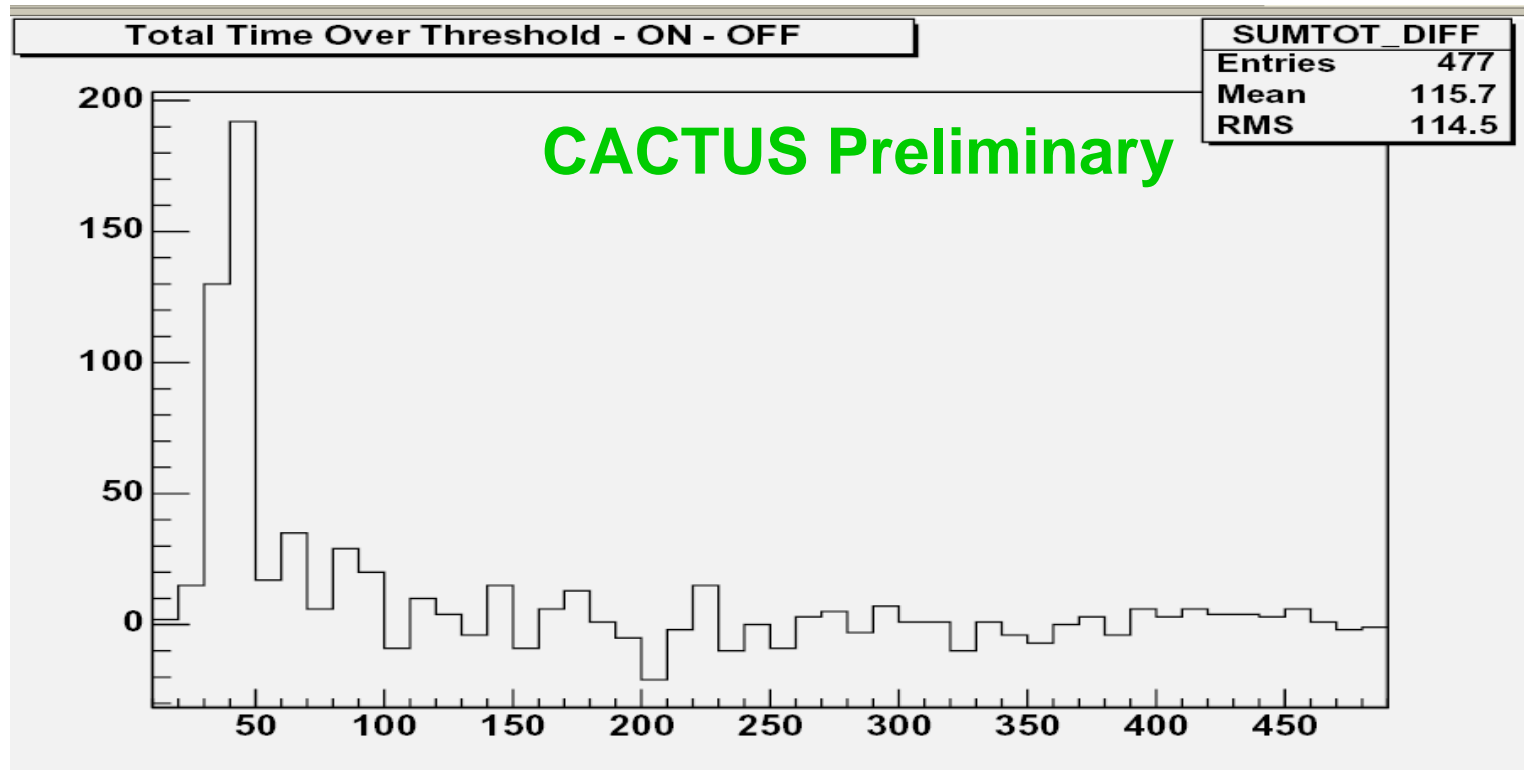
As an estimator of the energy spectrum of the excess in the Draco region, the pulse height distributions in the central region ($|RA| < 0.8$) minus the side-bands ($1.0 < |RA| < 1.8$) is plotted.

The peaked structure is mostly due to the detector resolution. At the present level of analysis it is difficult to distinguish a line-shape from an end-point Jacobian.



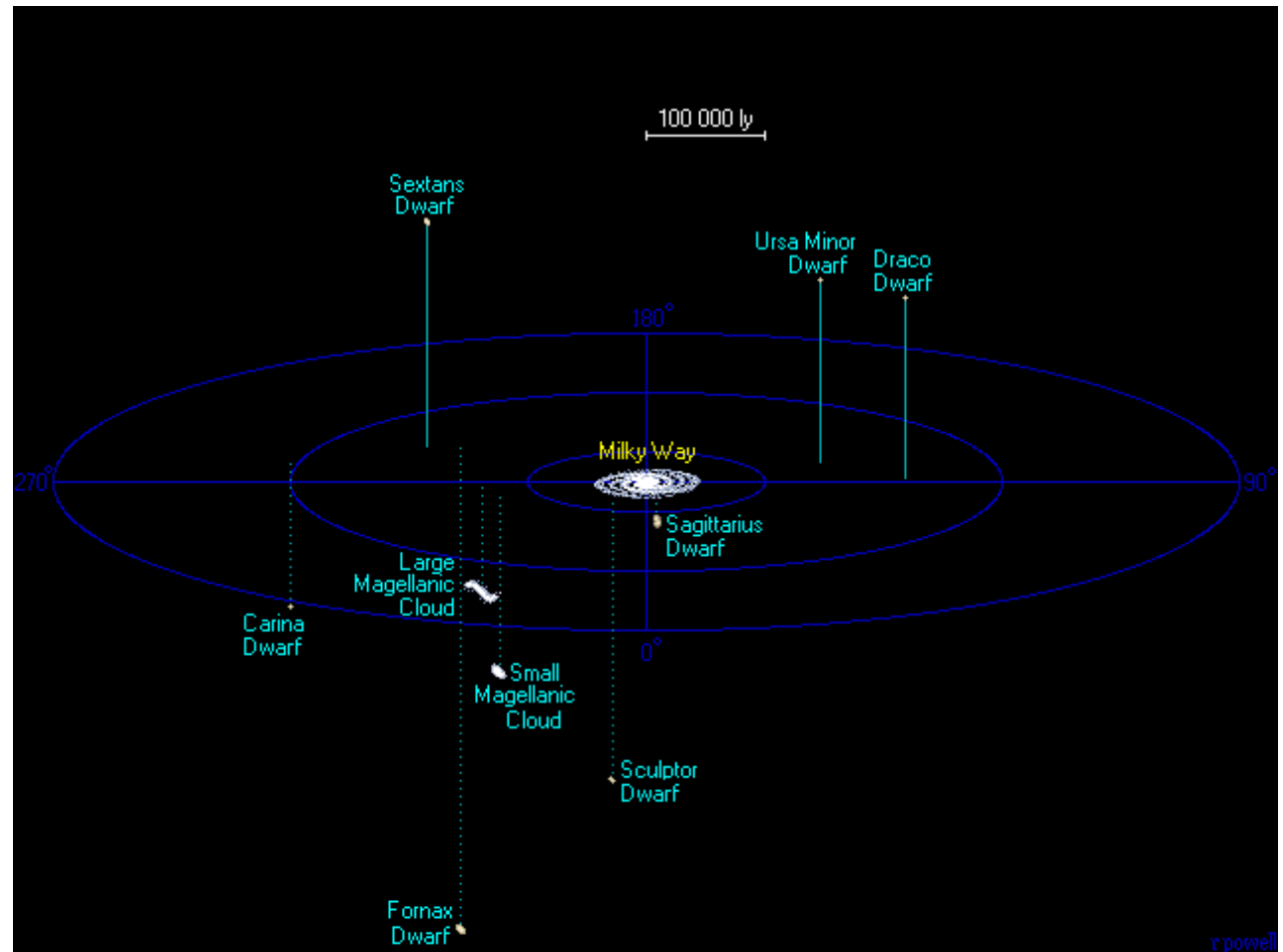
Improved energy definition using the shower-fitting method.

Example for one scan only.



Dwarf Spheroidal Survey

Our future plans include a survey of Sextans dwarf and a return to Draco in March 2006 to confirm the excess seen in this observing period.



Summary

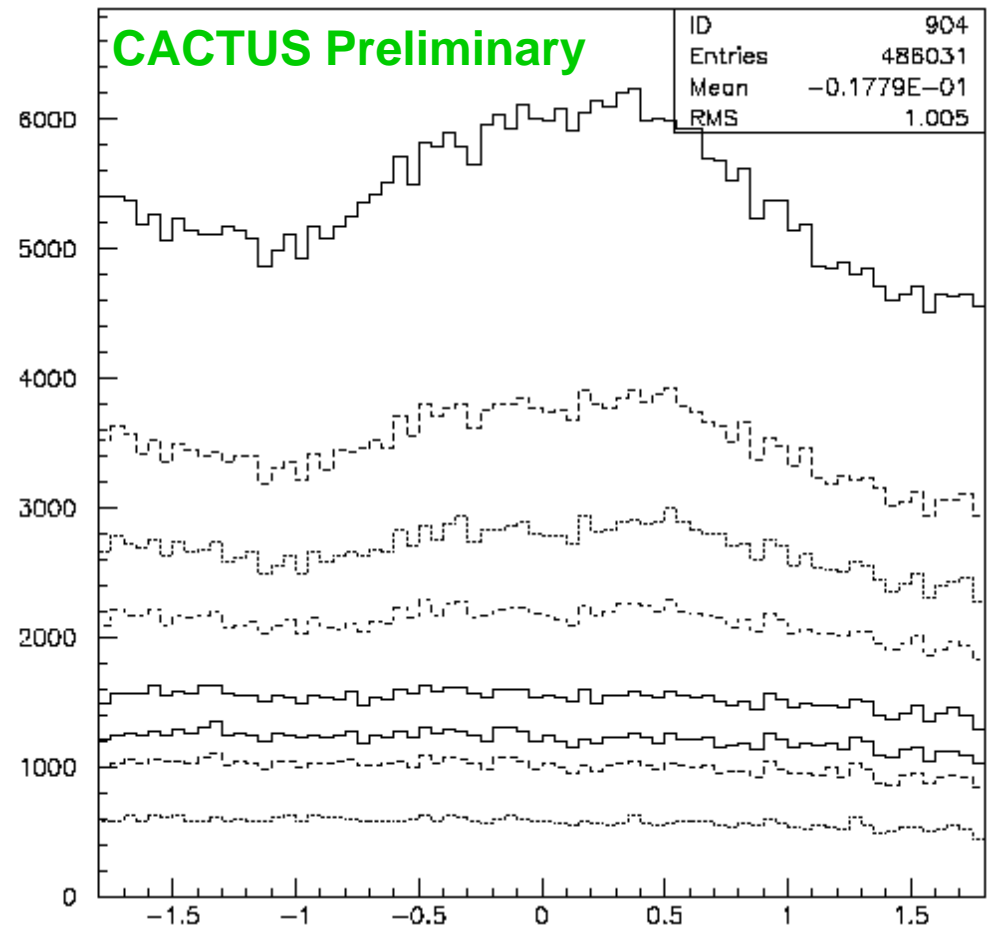
We have observed an excess of showers from Draco. We have to test the robustness of the excess. Work to be done:

1. Full shower fit analysis.
2. More detailed energy scale simulations and comparisons with world data on Crab.
3. Trigger threshold analysis.

Observe Sextans in the Fall.

Return to the Crab in the Fall for further calibration.

Implement time-imaging technique for improved gamma/cosmic ray discrimination.



Further update and published results expected by year end.

We welcome collaborators.

Acknowledgements

- We thank the Vice Chancellor for Research, Dr. Barry Klein, and the Dean for MPS, Dr. Winston Ko for critical support in the form of seed funds. We extend our gratitude to the Committee on Research at UC-Davis for a grant to implement our hardware at CACTUS.
- We thank the Office of the President of the University of California for supporting us with a grant for the development of the electronics for CACTUS.
- We are indebted to Southern California Edison, and Mr. Judd Kilminik in particular, for allowing us to use the Solar-2 site.
- An original grant from the Keck Foundation and Dr. Tumer from UCR paid for the mechanical and civil engineering aspects of converting Solar-2 into an ACT.
- The senior Electronics Engineer at UC-Davis, Mr. Britt Holbrook, takes a large part of the credit for the successful conversion and operation of CACTUS.
- We also wish to acknowledge the efforts of numerous undergraduate and graduate students who worked part time in the desert to make CACTUS into a reality.
- We are grateful to Prof. Alan Zych of UCR for loaning 50 phototubes to us.

Time-Projection Imaging

CACTUS records multiple hits and pulse-heights per Heliostat. The time-of arrival difference between these pulses can be correlated to height of emission.

$$\Delta h \sim c \Delta T / (n-1)$$

For, $|1-\beta| \sim |n-1| \sim 10^{-3}$

$$\Delta T = 16 \text{ ns} \Rightarrow \Delta h \sim 5 \text{ Km}$$

